Gray Wolf Optimization-Based Fractional-Order PID Controller for Synchronous Generator Voltage Regulation

Alemtsehay Hailu Abebe

A Thesis Submitted to

The Department of Electrical Power and Control Engineering

Collage of Electrical Engineering and Computing

Presented in Partial Fulfillment of the Requirement for the Degree of

Master's in Electrical Power and Control Engineering (Control Engineering)

Office of Graduate Studies

Adama Science and Technology University

June, 2025

Adama, Ethiopia

Gray Wolf Optimization-Based Fractional-Order PID Controller for Synchronous Generator Voltage Regulation

Alemtsehay Hailu Abebe

Advisor: Dr. Shimeles Demissie

Co advisor: Dr. Endalew Ayenew

A Thesis Submitted to

The Department of Electrical Power and Control Engineering

Collage of Electrical Engineering and Computing

Presented in Partial Fulfillment of the Requirement for the Degree of

Master's in Electrical Power and Control Engineering (Control Engineering)

Office of Graduate Studies

Adama Science and Technology University

June,2025

Adama, Ethiopia

DECLARATION

I hereby declare that this Master Thesis entitled "**Gray Wolf Optimization-Based Fractional-Order PID Controller for Synchronous Generator Voltage Regulation**" is my own work. That is, it has not been submitted for the award of any academic degree, diploma or certificate in any other university. All source of materials that are used for this thesis have been duly acknowledged through citation.

Name of the student	Signature	Date
---------------------------------	--------------------------	---------------------------

RECOMMENDATION

We, the advisors of this thesis, hereby certify that we have read the revised version of the thesis entitled "**Gray Wolf Optimization-Based Fractional-Order PID Controller for Synchronous Generator Voltage Regulation**." prepared under our guidance by **Alemtsehay Hailu s**ubmitted in partial fulfillment of the requirements for the degree of Mater's of science in Electrical Power and Control engineering (Control Engineering). Therefore, we recommend the submission of revised version of the thesis to the department following the applicable procedures.

Major Advisor	Signature	Date
-----------------------	-----------------------	---------------------
Co-advisor	Signature	Date
-----------------------	-----------------------	----------------------

APPROVAL PAGE

We, the advisors of the thesis entitled "**Gray Wolf Optimization-Based Fractional-Order PID Controller for Synchronous Generator Voltage Regulation**" and developed by **Alemtsehay Hailu**, hereby certify that the recommendation and suggestions made by the board of examiners are appropriately incorporated into the final version of the thesis.

Major Advisor	Signature	Date
-----------------------------	----------------------	----------------------
Co-advisor	Signature	Date
-----------------------------	----------------------	----------------------

We, the undersigned, members of the Board of Examiners of the thesis by **Alemtsehay Hailu** have read and evaluated the thesis entitled "**Gray Wolf Optimization-Based Fractional-Order PID Controller for Synchronous Generator Voltage Regulation**" and examined the candidate during open defense. This is, therefore, to certify that the thesis is accepted for partial fulfillment of the requirement of the degree of Master of Science in Electrical Power and Control Engineering.

______________________	________________	________________
Chairperson	Signature	Date
Dr.Negasa Muleta	[signature]	11/06/2025
Reviewer 1	Signature	Date
Dr Beteley Teka	[signature]	June 11, 2025
Reviewer 2	Signature	Date

Final approval and acceptance of the thesis is contingent upon the submission of its final copy to the Office of Postgraduate Studies (OPGS) through the Department Graduate Council (DGC) and Collage Graduate Committee (CGC).

______________________	________________	________________
Department Head	Signature	Date
______________________	________________	________________
Collage Dean	Signature	Date
______________________	________________	________________
Office of postgraduate studies, Dean	Signature	Date

ACKNOWLEDGEMENT

First, I would like to express my gratitude to God Almighty for granting me the strength, patience, and dedication to handle through this paper work. Next, I have great thanks to Adama Science and Technology University, mainly the Collage of Electrical Engineering and Computing, as well as the Power and Control Engineering department, for giving me this chance to be a part of the Master's program. And also, my deepest gratitude is extended to my advisor, Dr. Shimeles Demisie, and co-advisor, Dr. Endalew Ayenew, for their essential advice, priceless help, and constant inspiration have been of immeasurable value throughout the completion of this thesis. Additionally, I am grateful to prof. Gang GyooJin for generously sharing their extensive knowledge of MATLAB/Simulink.

Table of Contents

LIST OF FIGURES

LIST OF TABLES

LIST OF ACRONYMS

Abbreviations	**Description**
AVR	Automatic voltage regulator
EMF	Electromotive force
FOPID	Fractional order proportional integral derivative
GA	Genetic Algorithm
GWO	Grey wolf optimization
IAE	Integral of absolute error
IAEU	Integral of absolute error per unit control
IOPID	Integral order proportional integral derivative
ISE	Integral of squared error
ITAE	Integral of time absolute error
JSO	Jellyfish Search Optimizer
PI	proportional integral
PID	proportional integral derivative
PIDA	proportional integral derivative acceleration
PSO	Particle swarm optimization
SSA	Salp swarm algorithm
WOA	Whale optimization algorithms

ABSTRACT

Synchronous generators are crucial in power generation systems, which are used for converting mechanical power into electrical power with consistent frequency and voltage levels. In contemporary power systems, maintaining stable voltage levels in synchronous generators is paramount to ensuring reliable and efficient operation. Traditional PID controllers often struggle with the nonlinear dynamics and varying load conditions with these systems. To design a suitable controller, system modeling is required. In this regard, the linearized model of a synchronous generator can be developed. To keep the voltage regulation within minimum voltage deviation and improve the performance, a fractional-order Proportional-Integral-Derivative (FOPID) controller was implemented. To determine the optimal parameters for the FOPID controller, the Grey Wolf Optimization (GWO) algorithm will be utilized, which enhancing adaptability and control precision. Using these tuned parameters of the FOPID controller, the tracking performance is tested under different scenarios. The proposed GWO-FOPID controller performance is compared with, PID controller tuned using the Ziegler-Nichols method under both normal conditions and in the presence of step disturbances. Quantitative performance metrics showed that, although having a slightly earlier peak time of 0.928 s the FOPID controller had a faster settling time of 3.541s and significantly less overshoot of 11.397% than the PID controller with 4.1445s settling time and 46.676% overshoot. The result also showed a lower integrated absolute error with control effort (IAEU) of 2.5963 compared to 2.9865 for the PID controller. The results confirm that the GWO-optimized FOPID controller can enhance the synchronous generator voltage regulation.

Keywords: - Fractional Order PID (FOPID), Automatic Voltage Regulator (AVR), Grey Wolf Optimization (GWO), PID, Synchronous Generator, Optimization.

CHAPTER ONE

1.INTRODUCTION

1.1 Background of the Study

Synchronous generators are an essential component in power generation networks, which convert mechanical energy into electrical energy with persistent frequency and voltage levels. Synchronous generators (alternators) are the primary source of electrical power globally.Maintaining stable voltage regulation in synchronous generators is difficult due to factors like load fluctuations, external disturbances, and the intrinsic nonlinearity of power systems. Despite many studies conducted in the last decade, achieving optimal automatic voltage regulation for synchronous generators continue to present interesting problem. AVR system's is used to control the terminal voltage of generator, which enhances transient capability and guarantees power system stability during any external disturbance or parametric change(Ribeiro et al., 2015) .Effective voltage regulation is fundamental to achieving high power quality and reliability, both of them are essential for the efficient operation of power grids.

Maintaining a constant output voltage for a synchronous generator is achieved by the Automatic Voltage Regulator (AVR), which adjusts the excitation system's terminal voltage accordingly. In this manner, the field current of the generator is adjusted. Then this can be cause to alters the electromotive force (EMF) generated. The generator's power generation is changed to a new stable point while maintaining the intended terminal voltage(Özdemir & ÇELİK, 2017).However, an AVR system without controller's will response slowly and could become unstable.(Ibrahim et al., 2017). For AVR system a number of control strategy have been proposed and implemented. from these control strategies, the PID controller is most well-known that applied in industry. It is widely used since its simple and ease to implement. Manual regulation becomes highly complex within extensive interconnected power systems, require the implementation of automatic generation and voltage regulation. Therefore, AVRs are used at every generating station and synchronous generator to maintain a consistent generator output voltage. Typically, power factor, temperature, speed, and load change are the main causes of voltage instability.The equipment can be damaged due voltage changes in any way. Nevertheless, conventional PID controllers often struggle to cope with the complex dynamics and nonlinear behavior of synchronous generators, leading to sub-optimal performance (Ezenugu & Nwokonko, 2024).

Following the introduction of fractional calculus into control engineering, FOPID controllers have emerged as a prominent research area.Unlike integral order PID controllers, Fractional powers of integral and derivative terms define FOPID controllers. The controller's performance is determined by how effectively its parameters are tune when used in a particular process. The researchers have worked hard to minimize on the amount of time required on the selection of FOPID parameters, such as *KP, KI, KD,* λ and μ. When the plant order increase, become nonlinear so manually adjusting this controller parameters become complex. Tuning of these controller's parameters become quite simple after the emerging of fast and improved optimization algorithms (Bhullar et al., 2020).

In the last several years, meta-heuristic algorithms have become widely popular for tuning controller parameters. The Grey Wolf Optimization (GWO) algorithm is one of these algorithms that shows the most promise, by owing to its proficiency in identifying optimal solutions within complex, high-dimensional search spaces. Inspired by the social structure and hunting behavior of grey wolves, GWO provides an effective balance between exploration and exploitation and making it well-suited for tuning FOPID controller parameters to achieve desired voltage regulation performance. The wolf will attack the pray based on their fitness level. The GWO algorithm's hunting procedure adheres to the hierarchy level based on the wolves' fitness. The group leader, indicated by alpha (α), shares the highest level. The wolf, known as beta (β), represents the next level of the hierarchy, which is less powerful than the leader. Delta (δ), which represents the third level of the hierarchy, looks for the prey in directions other than α and β. The remaining wolves all belong to the omega (ω) level of the hierarchy, and their approach to the prey is determined by where the above hierarch is located(Verma et al., 2017).

1.2 Statement of the Problem

In modern power systems, maintaining stable and reliable voltage levels in synchronous generators is important for the performance and safety of electrical grids. Unregulated or fluctuating terminal voltage can face power quality issues, reduced efficiency, equipment damage, and instability in interconnected power networks. Sudden changes in load can have an effect of rapid variations in current and voltage at generator terminals, leading in voltage sags or spikes. Balancing transient stability with steady-state performance presents a significant challenge. Overly aggressive voltage regulation can lead to oscillations, while overly conservative control may result in sluggish response. PID controllers have been used extensively in the current generation for regulating the voltage of synchronous generators, but their effectiveness is undermined by their failure to respond dynamically to changing system dynamics and non-linearities found in synchronous generators. Apart from that, other controllers like sliding mode control used in the systems are bound to suffer from the chattering issue, leading to mechanical device wear and tear and poor performance. This thesis aims to design and optimize a Fractional Order PID(FOPID) controller for synchronous generator voltage regulation, using the Grey Wolf Optimizer (GWO) to enhance robustness, dynamic performance, and tuning efficiency. Despite their advantages, FOPID controllers design needs careful tuning of parameters, which can be complicated due to the high dimensional of the search area and the non-linear nature of the objective functions involved. To optimize the parameters of a controller we used meta-heuristic algorithms; however, many existing approaches often face challenges such as slow convergence rates and addressing the susceptibility to local optima convergence, the Grey Wolf Optimizer (GWO) algorithm emerges as a robust alternative, recognized for its proficient exploration and exploitation functionalities.

1.3 Research Question

- The following main research questions are intended to be addressed by this work:

  1. How can a Fractional-Order PID (FOPID) controller improve performance of voltage regulation in asynchronous generator compared to conventional PID controllers?

  2. How effectively does the Grey Wolf Optimization algorithm determine optimal FOPID controller parameters for enhancing voltage regulation in synchronous generators?

  3. What performance improvements, in terms of response time, and voltage deviation, can be seen when simulating a GWO-optimized FOPID controller in MATLAB/Simulink?

1.4 Objective

1.4.1 General Objective

This research aims to develop a GWO-optimized FOPID controller for synchronous generator voltage regulation and evaluate its performance in comparison to traditional PID through simulation and stability analysis.

1.4.2 Specific Objectives

- Develop a comprehensive mathematical model of a synchronous generator, represent its dynamic behavior and the factors affecting voltage regulation.
- Design a FOPID controller suitable for synchronous generator voltage regulation.
- Implement the Grey Wolf Optimizer algorithm for FOPID controller parameters tuning.
- Test the performance of the proposed controller using MATLAB/Simulink simulations and compare its performance with the conventional PID controller.

1.5 Significant of the Study

Since synchronous generators is crucial in maintaining power grid stability, precise voltage regulation is essential. This research overcome the challenge faced by unregulated terminal voltage of synchronous generator by proposing fractional-order PID(FOPID) controller tuned by Grey Wolf Optimization (GWO). FOPID controllers have greater flexibility for voltage regulation than that of conventional PID controllers. GWO algorithm can be anticipated to yield better outcomes in FOPID parameter optimization due to its exploration and exploitation capacity. By evaluating the proposed controller's performance in MATLAB/Simulink simulations, focusing on response time, voltage deviation, and overall system robustness, this research aims to significantly improve voltage regulation in synchronous generators.

1.6 Scope of the Study

This research aims to implementing a fractional-order PID (FOPID) controller optimized by Grey Wolf Optimization to maintain the terminal voltage of a synchronous generator at a given desired value. The study includes mathematical modeling of the plant, controller design, parameter optimization using GWO, and simulation-based evaluation. The performance of the GWO-based FOPID controller will be compared with PID controller in terms of voltage deviation, performance metrics, and robustness to disturbances.

1.7 Limitation of Study

This thesis research limited to theoretical design, in the sense that the performance of the proposed FOPID controller is evaluated solely by simulation, without implementation on a grid-connected synchronous generator model subject to realistic conditions.

1.8 Thesis Organization

This research thesis is organized as follows:

In the chapter one explains the background of synchronous generator voltage regulation, scope, significant, limitation, statement of problem and research objective. Following the Introduction, in chapter two, describes a literature review of the voltage regulation of synchronous generator and FOPID controller and also previous works which are directly related to the idea of this thesis work. The material and methods utilized to complete this research project are cover in chapter 3, as well as the mathematical modeling of synchronous generator and AVR. In chapter four the controller design is discussed briefly and also its optimization methods. Chapter five presents the results and discussion of the simulation. Lastly, the research work's conclusion and recommendation are found. Additionally, several recommendations for extensions to possible areas of future study are made.

CHAPTER TWO

2.LITRATURE REVIEW

2.1 Overview

The synchronous generator in a power system may oscillate around the equilibrium point when disturbance such as shift in load or fluctuation in the turbine output takes place(Li et al., 2017).Voltage regulation is essential in synchronous generator to ensure power quality, stability and reliability within electrical grids. In the field of power systems, generator excitation control is an important subject. Good excitation control plays a highly efficient and supportive role in improving transient stability and consequently reducing voltage oscillations within a power system.An essential part of power systems that use excitation control to adjust voltage is the automated voltage regulator (AVR). The Automatic Voltage Regulator precisely adjusts the excitation system's terminal voltage to maintain the generator's output or terminal voltage constant. In this manner, the field current of the generator is adjusted. Additionally, this situation alters the electromotive force (emf) that can be generated. While the terminal voltage is maintained at the correct level and the generator's power generation is changed to a new stable point, an AVR system without a controller will respond slowly and could lead to instability(Ezenugu & Nwokonko, 2024). Proportional-Integral-Derivative (PID) controllers are extensively employed in industrial process control due to their simple design and effective performance, characterized by low overshoot and quick settling times for slower processes.

2.2 Theoretical Background of Synchronous Generator Voltage Regulation

A synchronous generator (alternator) is an electrical device that used to converts mechanical energy into electrical energy depending on the principle of electromagnetic induction. The electric energy we used in our home or industries is mostly produced by the synchronous generator. Among the various global energy conversion technologies, synchronous generators stand out as the primary converters of most energy.In electric power systems, synchronous generators are made for nominal or rated voltage. In real-world applications, disturbances such as variations in loads and variations in turbine output would affect the synchronous generator's condition and cause it to oscillate around the equilibrium state. Consequently, these oscillations cause the generator terminal voltage to deviate from its desired constant level. This damages the power system's stability and degrades power quality.(Hekimoğlu, 2019) .Voltage regulation in a synchronous generator is vital in order to maintaining stable power supply by ensuring a constant terminal voltage under load variation (Hadi Saadat, 1999).It is defined as:

$$\text{Voltage regulation}(\%)=\frac{E_{\text{no load}}-E_{\text{full load}}}{E_{\text{full load}}}\times 100\% \tag{2.1}$$

<u>Where:</u>

- $E_{no\ load}$ = Open circuit voltage (no load)
- $E_{full\ load}$ = Terminal voltage at full load

2.2.1 The Main Component of Synchronous Generator

A synchronous generator is electric device that contain several components used to transform mechanical energy into electrical energy. These components include:

Stator: is the non-rotating part of the generator with the armature winding, which produces the output AC voltage. It is built with laminated iron cores to reduce eddy current losses and improve efficiency. Stator windings are located in slots to give a three-phase AC output.

Rotor: is the moving part and produces a rotating magnetic field. It is guided by a prime mover (such as a diesel engine, steam turbine, or hydro turbine) that is mechanically connected to it. There are two types of rotors. One is the salient pole rotor (used in low-speed application such as hydro generators) and the other one is cylindrical rotor (used in high-speed applications like steam turbines).

Field Winding: The rotor's field winding creates the required magnetic field by being stimulated by a DC source. Excitation can be externally provided or via a self-excited arrangement depending on the exciter types.

Armature Winding: is responsible for generating the induced AC voltage by utilizing the rotor's revolving magnetic field. It supplies the stator-mounted external load to deliver electrical power.

Exciter: it provides the DC supply needed to the field winding. It may be an independent DC generator or an electronic excitation system employed to regulate the field current.

Automatic Voltage Regulator (AVR): it regulates the field current to provide a constant terminal voltage. Accordingly, by modifying the excitation based on the load requirement, it control the output voltage.

Bearings and Shaft: rotor is mounted on a shaft, supported by bearings, which allows smooth rotation with minimal friction.

2.2.2 Working Principle of Synchronous Generator

Synchronous generators operate according to Faraday's laws of electromagnetic induction, which state that rotating an armature coil within a uniform magnetic field induces an electromotive force. In a similar manner, if the conductor is stationary and the magnetic field rotates, EMF may be produced. When the revolving magnetic field cuts the stator winding's it creates alternating voltage. The frequency of the generated voltage relies on the rotor speed and number of poles:

$$f = \frac{PN}{120} \tag{2.2}$$

Where**f** is frequency (Hz), **P**is number of pole and **N**is speed in RPM.

2.2.3 Component Affecting Voltage Regulation

2.2.3.1 Field Excitation

The excitation system is crucial to providing the field current for the generator’s rotor winding. Under various load circumstances, the AVR regulates the excitation to keep the terminal voltage steady.

Field Winding Resistance and Reactance (Rf,Xf): Affects the rotor magnetic field response.

Exciter Dynamics: The exciter provides controlled DC voltage to the rotor, influencing voltage stability.

AVR Response Time: A slow AVR will add oscillations, while a well-tuned AVR gives steady voltage regulation.

2.2.3.2 Armature Reactance (R_s) and Resistance (X_s)

Armature reactance and resistance can affect the voltage drop in the machine. At different loads high reactance leads to high voltage fluctuation.

Synchronous Reactance (X_s): Elevated reactance increases internal voltage drop, affecting regulation.

Armature Resistance (R_s): Influences losses and contributes marginally to voltage drop.

2.2.3.3 Load Power Factor

The operating power factor significantly influences a synchronous generator's voltage regulation: it is often negative for leading power factors, quite high for lagging power factors, and modest for that of unity power factor(Stephen J. Chapman, 2005).

Unity power factor: the phase and terminal voltage will exhibit a minor drop.

Lagging (Inductive Load): Causes voltage drop due to increased reactive power demand.

Leading (Capacitive Load): Increases terminal voltage due to reactive power injection.

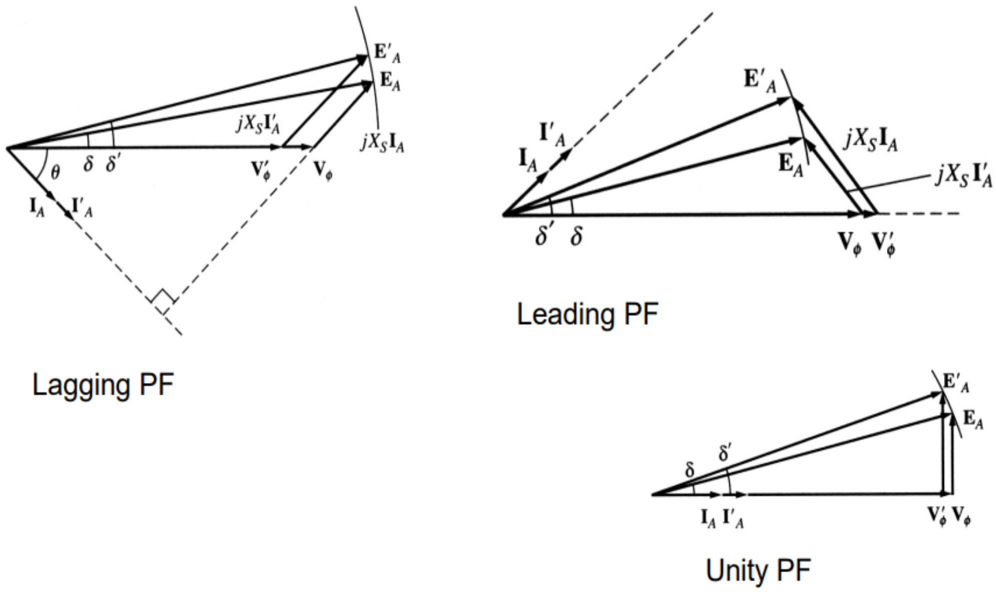

Figure 2. 1: Impact of increased generator load on terminal voltage(Stephen J. Chapman, 2005)

2.2.4 Automatic Voltage Regulation

Reactive power control in generators is principally achieved through the regulation of generator excitation, typically using an automatic voltage regulator(Hadi Saadat, 1999). An AVR is responsible for keeping the magnitude of synchronous generator's terminal voltage constant at a specified level. The Automatic Voltage Regulator controls the output voltage of generator, thereby regulating bus voltage by adjusting reactive power. This is achieved by continuously monitoring the terminal voltage, rectifying and filtering the signal, and comparing it to a reference value. The voltage error is amplified and fed back to adjust the alternator's field excitation. This excitation system, by manipulating the generator's field current, effectively achieves and maintains terminal voltage regulation. The Automatic Voltage Regulator (AVR) continuously monitors, rectifies, and smooths the terminal voltage, comparing it to a reference input. Consequently, the amplified error signal causes the exciter to increase the generator's field voltage. For example, a reactive power load increase causes a terminal voltage drop. This drop is sensed, corrected, and compared to a setpoint. The exciter then uses the amplified error signal to raise its field and terminal voltages, which raises the output of reactive power and created electromagnetic field, bringing the terminal voltage back to the desired level.

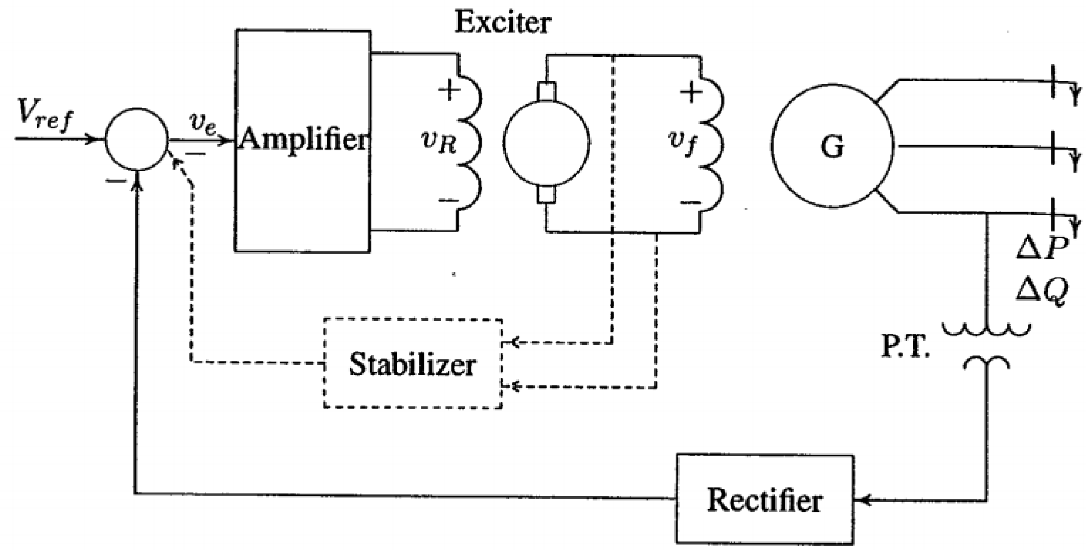

Figure 2. 2 : Typical Configuration of an Automatic Voltage Regulator System(Hadi Saadat, 1999)

2.2.4.1 Main Component of AVR

Regulator (Amplifier): it compares the desired and actual excitation currents, then amplifies input control signals to suit the exciter's requirements.

Exciter: feeds the synchronous generator's field winding with the field current. By controlling this current, the exciter directly manages the magnetic flux, consequently regulating the generator's voltage output.

Generator: the machine magnetization curve determines the synchronous machine generated emf, and the generator load affects the terminal voltage.

Potential Transformer: measures the terminal voltage of the generator and then give feedback to the AVR system for voltage regulation.

Rectifier: it senses the terminal voltage of generator’s, rectifies the AC signal into DC, and then compares it with a reference representing the desired terminal voltage.

2.3 Overview of Fractional Order PID controller

Fractional calculus, as introduced by Podlubny (1999), emerged as a method to significantly improve the versatility of tuning, robustness, and frequency response characteristics of conventional PID controllers. FOPID controllers are increasingly used, namely the $PI^{\lambda}D^{\mu}$ controller, in industries due to the substantial benefits gained from their two extra parameters, which offer greater flexibility for improving control system performance. The fractional PID controller is an extension of conventional PID controller. The FOPID controller is employed as a regulatory mechanism to augment the system's dynamic characteristics and minimize any steady-state error(Mohammad Ali Daftari & Mohammad Ali Nekoui, 2018). Figure 2.3 shows the block diagram of the fractional-order PID controller.

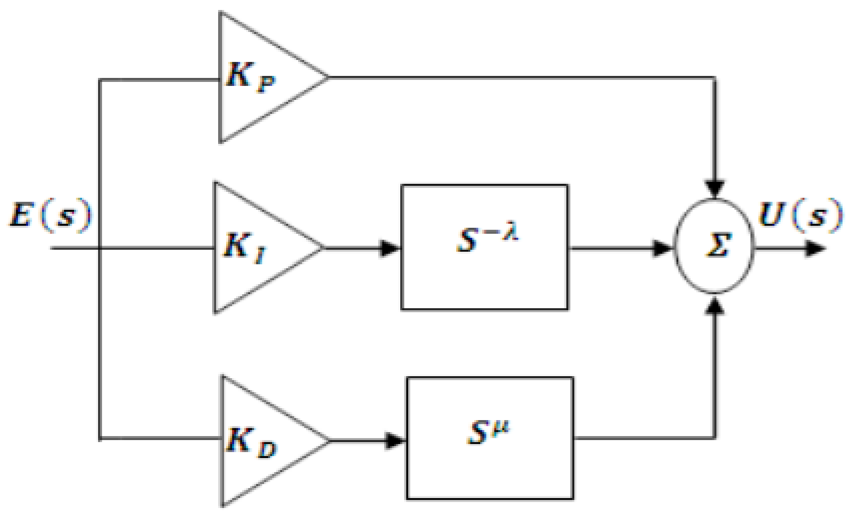

Figure 2. 3:Fractional Order PID controller Diagram*(babu & Chiranjeevi, 2016)*

This is the transfer function form of $PI^{\lambda}D^{\mu}$-controller:

$$G(s) = \frac{U(s)}{E(s)} = K_p + K_i s^{-\lambda} + K_d s^{\mu} \tag{2.3}$$

FOPID controllers are mostly used topics to study as they are enhanced flexibility and performance over traditional PID controllers. There are several Recent studies that explore various applications and optimization techniques for FOPID controllers. some of the most interesting research papers are:

(Abbas et al. ,2024)Propose a self-adaptive based fractional-order PID (FOPID) controller to maintain optimal particle velocity within pneumatic conveying systems. The proposed method used an optimization technique to tune FOPID parameters, that improved system performance under varying load conditions. The study compares the FOPID controller with conventional PID and other control strategies, demonstrating its superiority based on stability, accuracy, and adaptability. The results show that the self-adaptive optimized FOPID controller parameters enhance the robustness and efficiency of pneumatic systems, making it an acceptable solution for industrial applications.

The application of the Jellyfish Search Optimizer algorithm for the optimal design and tuning of a fractional-order PID controller for a paper machine headbox was proposed by (Nataraj & Subramanian, 2025). This paper explores the application of the JSO for tuning an FOPID controller in a paper machine headbox system, which is crucial for maintaining uniform paper quality. The study concludes that the JSO-optimized FOPID controller has widespread use in improving system response by decreasing the rise time by 25%, settling time by 30%, and maximum overshoot by 20% compared to normal PID controllers. The findings demonstrate the Jellyfish Search Optimizer's (JSO) effectiveness in optimizing FOPID controller parameters for industrial process control.

2.4 Grey Wolf Optimization

Grey Wolf Optimization (GWO) is a metaheuristic algorithm inspired by nature that imitates the hunting habits and leadership structure of grey wolves. It is widely used for tuning controllers, including Fractional Order PID (FOPID) controllers, to improve steady state and dynamic performance(Mirjalili et al., 2014).

2.4.1 Working Principle of GWO for FOPID Tuning

Initialization: Initially population of grey wolves (candidate FOPID parameter sets) is randomly generated within predefined limits of the given parameters.

Hierarchy Formation: In this hierarchy, the alpha (**α**) wolf represents the best fitness solution**,** followed by beta (**β**) as the second best, and delta (**δ**) as the third best. All other solutions are classified as omega (**ω**) wolves**.**

Hunting Process:

1. The wolf's positions will shifts depend on the top three solution according to the encircling mechanism and adaptive coefficients**.**
2. The phase of exploration and exploitation guide the wolves to the optimal tuning parameters.

Termination: The loop run until termination condition met (e.g., a predefined number of iterations or convergence).

2.4.2 Fitness Function for FOPID Tuning

The performance of a given FOPID controller configuration is quantified by a fitness function. Common performance indices include integral of absolute error (IAE), integral of squared error (ISE), integral of time-weighted absolute error (ITAE) and integral of time-weighted squared error (ITSE).

$$
\begin{aligned}
IAE &= \int_0^\infty |e(t)|\,dt \\
ISE &= \int_0^\infty e^2(t)\,dt \\
ITAE &= \int_0^\infty t\,|e(t)|\,dt \\
ITSE &= \int_0^\infty t e^2(t)\,dt
\end{aligned}
\tag{2.4}
$$

Where e(t) is the error signal. The GWO algorithm minimize one of these objective functions to fine tune FOPID gains (K_p, K_i , K_d , μ , λ).

2.5 Related work on AVR of Synchronous Generator

While synchronous generators are designed for nominal voltage operation, real-world disturbances like load changes and turbine output fluctuations can disrupt their stability, causing them to oscillate around their equilibrium state. As a direct result of these oscillations, the generator terminal voltage cannot be maintained at a constant level, which in turn compromises the power system's stability and diminishes overall power quality.(Hekimoğlu, 2019). In synchronous generators, magnetic saturation, armature reaction, and thermal effects often introduce nonlinearities that impact voltage regulation. Traditional controllers struggle to maintain stable voltage for combined dynamic load change. For example, sudden load increases can lead to voltage instability due to non-proportion excitation responses under saturation.When an imbalanced load is present, negative sequence currents flow through a synchronous machine's stator windings, creating a magnetic flux that rotates at twice the rotor angular velocity. Additional losses are caused by the double frequency currents that are induced in the rotor winding by this flux. Additionally, a double-frequency electromagnetic torque pulsing is produced, resulting in harmonic distortions of the stator and rotor voltages and currents and extra vibrations. (Bulatov et al., 2023; Karakaya et al., 2023).

The research works by (Türksoy & Türksoy, 2024)aims on developing sliding mode controller for Automatic Voltage Regulation of power systems. AVR systems adjust the terminal voltage of synchronous generator’s in order to maintain reactive power balance; however, the reliability of voltage regulation is challenged due to rapid networking of renewable energy sources. this study proposes a quick and stable sliding mode controller, to eliminate the issues stated above. since real controllers have maximum and minimum limits which can affect performance, it is impossible to simulate the exciter without considering the factor of saturation due to potential chattering problems, and also the mathematical models can potentially reduce transient performance, they do not absolutely define real system complexity. In general, the study highlights the need for advanced control methods to improve voltage regulation with renewable energy integration.

Fractional calculus, as introduced by Podlubny (1999), emerged as a method to significantly improve the versatility of tuning, robustness, and frequency response characteristics of conventional PID controllers. In recent times, metaheuristic algorithms have emerged as efficient tools for tackling numerous optimization challenges. They offer several advantages over a number of traditional approaches due to their ability to solve problems and provide nearly optimal solutions without going into great detail into the problem concepts(Oladipo et al., 2020).Many researchers have investigated voltage regulation of synchronous generators using PID and fractional-order PID (FOPID) controllers. Let's explore some of their findings.

(Salih et al., 2019) works on enhancing synchronous generator voltage regulation through a PSO-optimized PID-ANN controller. since the conventional PID controllers cause instability and difficulty in handling nonlinearities, the proposed controller can address this limitation. The simulation results indicate that improved performance when compared to conventional controllers. However, challenges like high gain instability, nonlinear system dynamics, and practical limitations on output voltage magnitude remain.

(Anwar et al., 2021) proposes optimizing a PID controller for voltage regulation using Chaotic Particle Swarm Optimization (CPSO). By integrating chaotic behavior within PSO algorithm, the proposed methods focus to improve convergence speed and its accuracy. The effectiveness of CPSO in finding optimal PID parameter value is depicted using simulations, which demonstrate improved performance compared to other optimization techniques. While the proposed CPSO-tuned PID controller shows promising results, further research is needed to indicate its effectiveness in handling complex system dynamics, assess its robustness to parameter variations, by integrating it with advanced control techniques.

In (Li et al., 2017) research work, a novel design strategy for fractional-order PID (FOPID) controllers in Automatic Voltage Regulator system’s, utilizing a bode reference model was proposed. The FOPID parameters are adjusted by determining the solution that minimizes the Integrated Absolute Error (IAE) as objective function. Tuning is achieved with the Particle Swarm Optimization (PSO), which is prone to slow convergence and local optima issues, especially for large and complex systems like synchronous generators. PSO can sometimes converge prematurely or get stuck in local optima, affecting controller robustness. (Mosaad et al., 2019), Whale Optimization Algorithm (WOA) used to tune the parameters of PID and PIDA controller’s for Automatic Voltage Regulator (AVR) systems were also proposed. Optimized controllers provide improved robustness and stability compared to the traditional approach, especially in cases of load variation. While their proposed strategy reduces some of the stability issues, it is also subject to issues of time delay, nonlinear loads, and changing operating points depending on the intrinsic weaknesses of PID and PIDA controllers. Additionally, the WOA algorithm might focus on specific performance indices, potentially compromising other aspects of the controller's performance, such as rise time and bandwidth.

In research work by (Khan et al., 2019)a fractional order PID controller for AVR systems is presented. The Salp Swarm Optimization method is used to optimize the FOPID controller parameters. The suggested approach improves stability and dynamic response. Nevertheless, this paper has certain limitations, which are Large overshoots and settling times can happen, the optimization algorithm may become stuck in local solutions, and there is a chance that equipment may be impacted by an unstable power supply.

An enhanced FOPID controller for AVR systems, optimized with an improved Marine Predators Algorithm was presented by (Mohd Tumari et al., 2023).This research work investigates the application of fractional calculus in dynamic systems, depending on their advantages in modeling complex behaviors. It briefly describes mathematical formulations, and numerical algorithms with the real-world applications. This study demonstrates the way in which fractional-order control methods enhance system performance in all areas of engineering. The results confirm the effectiveness of the fractional calculus towards better description of system dynamics, making them effective to use in control and signal processing.

In General, the literature review discovers a number of the drawbacks of the current voltage regulation approaches for synchronous generators, especially those that depend on fractional-order PID (FOPID) and conventional PID controllers. Under the situation of complex systems and varying operating conditions, such controllers tend to face nonlinearities, sluggish convergence, and local optimum problems. In order to address the above limitation, this thesis propose FOPID controller tuned by Grey Wolf Optimization (GWO) By having the capability to escape local optima and enhance convergence speed, GWO algorithm has the potential to offer an improved performance and more robust solution for synchronous generator voltage regulation.

CHAPTER THREE

3.MODELING OF SYSTEM DYNAMICS

3.1 Introduction

In this chapter, discuss in detail the methodology, including the materials and methods used in this research, develop a comprehensive dynamic model of the synchronous generator.

3.2 Materials used for the Study

MATLAB/SIMULINK software package will be used for simulation to test and analysis the system model of this thesis. This software is the general-purpose computing software which consists a broad range of many toolboxes. It has a high-level mathematical package design for doing numerical solutions and graphical user interfacing. Also, MS-Office will be used to write the whole documentation rather than equations and MATHTYPE will be to write the equations or formulas.

3.3 Methods to Follow

Figure 3.1 illustrates how the necessary task was completed for this research study. The study will utilize the following methods and techniques to fulfill its general and specific objectives. First, begin with defining the problem, followed by collecting relevant data and conducting a literature review to identify research gaps. Next, the requirements are specified, and the collected data is analyzed mathematically. A dynamic model is then developed and a controller is designed. The designed controller is implemented on the dynamic model using MATLAB/Simulink software, followed by simulation and testing of the solution. If the solution meets the specified requirements, a conclusion and recommendation are drawn. However, if the solution does not meet the requirements, the process loops back to the stage of developing the dynamics modeling and designing the controller.

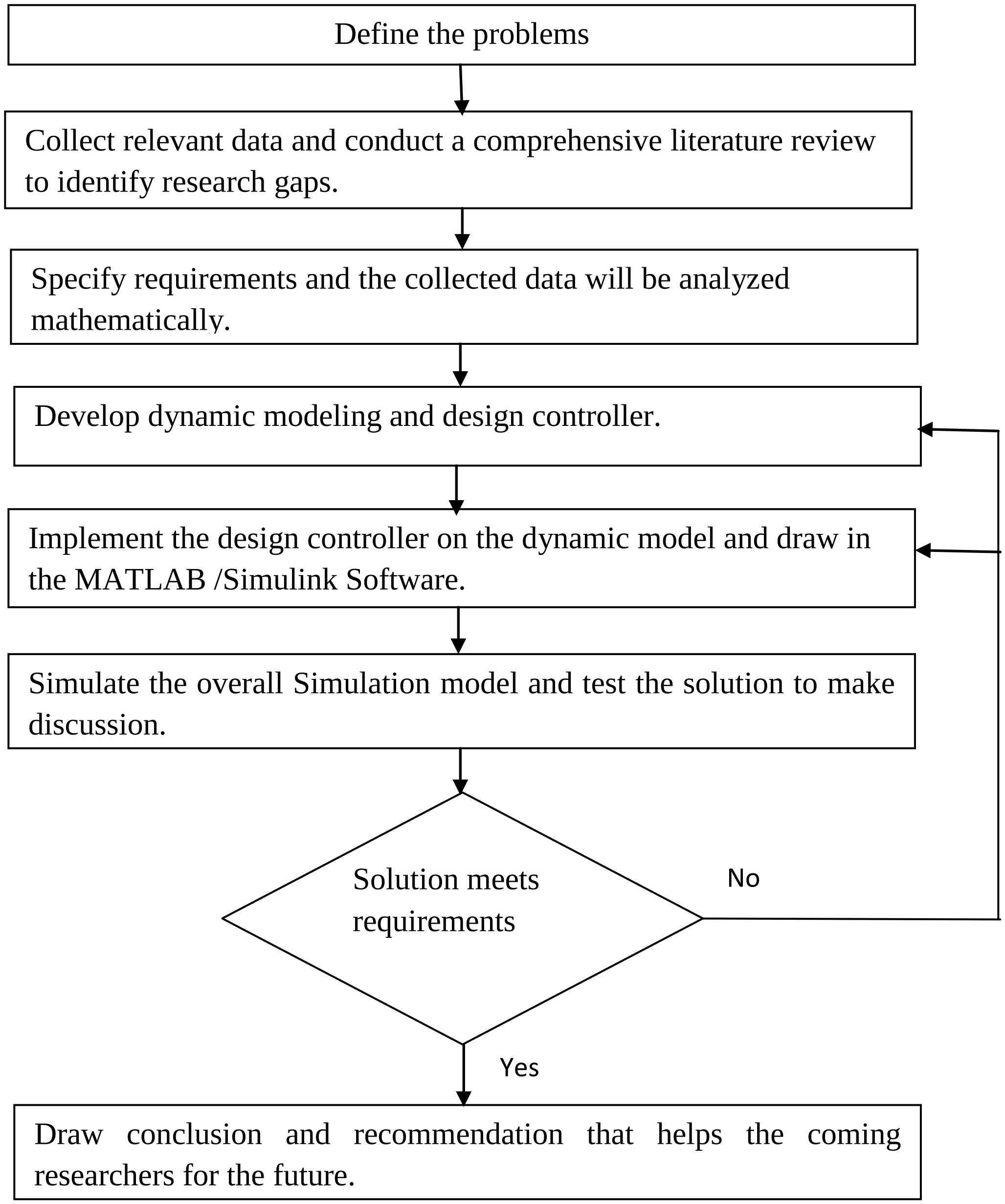

Figure 3. 1:Work flow of the thesis

3.4 General Block Diagram of the System

Figure 3.2 illustrates the general block diagram of the suggested system designed to control system trying to keep a generator output voltage steady, where the reference input voltage (V_{ref}) is compared with the feedback voltage (V_s) from sensor to generate an error signal (V_e). Here the controller (FOPID) is utilize to adjust the generator setting to maintain the desired terminal voltage. Consequently, to ascertain the optimal parameters for the controller GWO optimization algorithm is used.

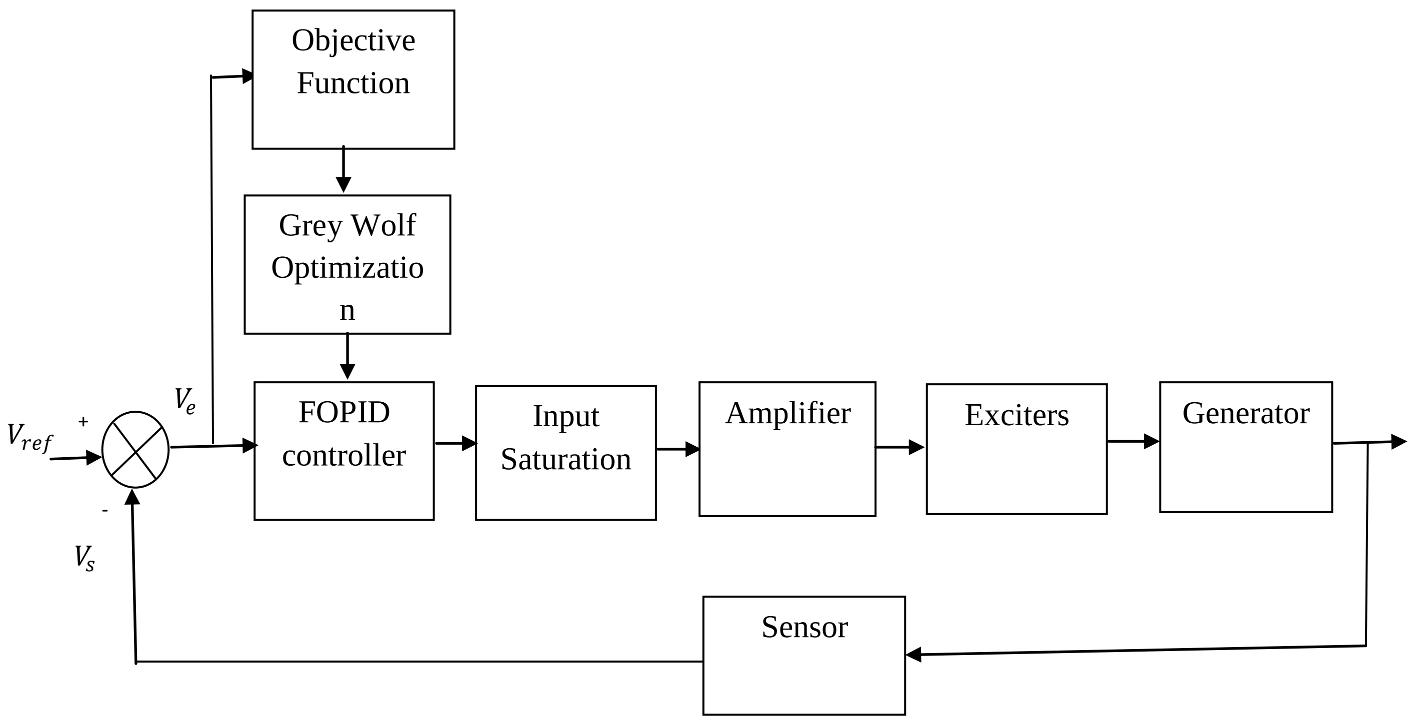

Figure 3. 2:Overview of the proposed system's block diagram

3.5 Mathematical Modelling of Synchronous Generator

Synchronous machines typically contain three windings on the stator and one field winding on the rotor. To accurately model the behavior of the rotor's short-circuited damper windings, two additional conceptual windings are often introduced along the direct and quadrature axes. The dynamic characteristics of a synchronous generator is effectively described using three main sets of equations. From Figure 3.3 we derive basic electrical equation of synchronous generator. Before proceeding to equation, we note that positive polarity for stator current is taken as outward from the machine. Conversely, the positive direction for both field and amortisseur currents is considered inward(Brezovec et al., 2022; KUNDUR, 1994).

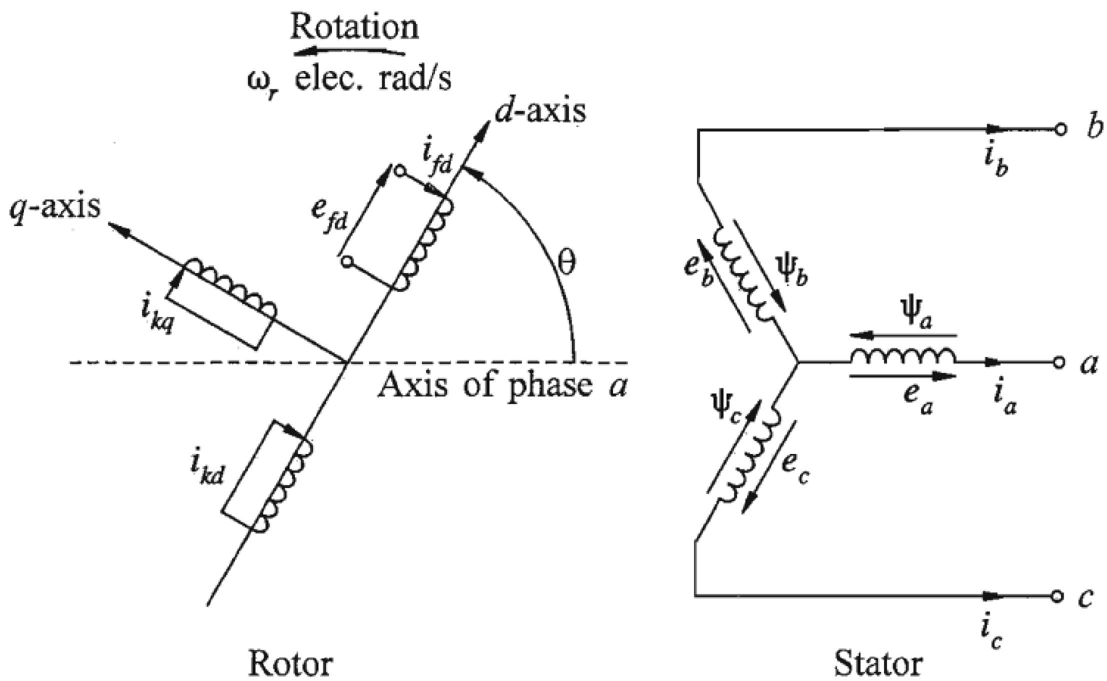

Figure 3. 3:Equivalent circuit of synchronous generator(KUNDUR, 1994)

3.5.1 Circuit Equation of Stator

The three phase voltage equation are:

$$e_a = \frac{d\varphi_a}{dt} - R_a i_a \quad (3.1)$$

$$e_b = \frac{d\varphi_b}{dt} - R_a i_b \quad (3.2)$$

$$e_c = \frac{d\varphi_c}{dt} - R_a i_c \quad (3.3)$$

and the linkage flux in the three-phase winding are given by:

$$\varphi_a = -l_{aa} i_a - l_{ab} i_b - i_{ac} i_c + l_{afd} i_{fd} + l_{akd} i_{kd} + l_{akq} i_{kq} \quad (3.4) \qquad \varphi_b = -l$$

$$\varphi_c = -l_{ac} i_a - l_{bc} i_b - i_{cc} i_c + l_{cfd} i_{fd} + l_{ckd} i_{kd} + l_{ckq} i_{kq} \quad (3.6)$$

self-inductance l_{aa} defined as the ratio of the magnetic flux linking phase 'a' winding to the current i_a,assuming zero current in all other circuits.

$$\begin{aligned} l_{aa} &= L_{a1} + l_{gaa} \\ &= L_{a1} + L_{g0} + L_{aa2}\cos 2\theta \\ &= l_{aa0} + l_{aa2}\cos 2\theta \end{aligned} \tag{3.7}$$

Due to symmetrical arrangement where phase b and c winding are identical to phase a and offset by 120 and 240 degree respectively, we have

$$l_{bb} = L_{aa0} + L_{aa2}\cos(\theta - \frac{2\pi}{3}) \tag{3.8}$$

$$l_{cc} = L_{aa0} + L_{aa2}\cos 2(\theta + \frac{2\pi}{3}) \tag{3.9}$$

The mutual inductance between phase a and b defined as:

$$l_{ab} = l_{ba} = -L_{ab0} - L_{ab2}\cos(2\theta + \frac{\pi}{3}) \tag{3.10}$$

Similarly,

$$l_{bc} = l_{cb} = -L_{ab0} - L_{ab2}\cos(2\theta - \pi) \tag{3.11}$$

$$l_{ca} = l_{ac} = -L_{ab0} - L_{ab2}\cos(2\theta - \frac{\pi}{3}) \tag{3.12}$$

The mutual inductance and the flux connecting the two winding are at their maximum if the stator and rotor windings are aligned. There is no flux connecting the two circuits when the two windings are 90 degrees apart, and there is no mutual inductance.

$$l_{afd} = L_{afd}\cos\theta \tag{3.13}$$

$$l_{akd} = L_{akd}\cos\theta \tag{3.14}$$

$$l_{akq} = L_{akq}\cos(\theta + \frac{\pi}{2}) = -L_{akq}\sin\theta \tag{3.15}$$

In order to determine the mutual inductance, present between phase b winding and the rotor circuits, θ is replaced by $\theta - \frac{2\pi}{3}$; for phase c winding θ is changed by $\theta + \frac{2\pi}{3}$. Now substitute Equation from (3.7) up to (3.15) into Equation (3.4) to (3.6), we obtain

$$\varphi_a = -i_a[L_{aa0} + L_{aa2}\cos 2\theta] + i_b[L_{ab0} + L_{aa2}\cos(2\theta + \frac{\pi}{3})]$$
$$+i_c[L_{ab0} + L_{aa2}\cos(2\theta - \frac{\pi}{3})] + i_{fd}L_{afd}\cos\theta \quad (3.16)$$
$$+i_{kd}L_{akd}\cos\theta - i_{kq}L_{akq}\sin\theta$$

$$\varphi_b = -i_a[L_{ab0} + L_{aa2}\cos 2(\theta + \frac{\pi}{3})] - i_b[L_{aa0} + L_{aa2}\cos 2(\theta - \frac{2\pi}{3})]$$
$$+i_c[L_{ab0} + L_{aa2}\cos(2\theta - \pi)] + i_{fd}L_{afd}\cos(\theta - \frac{2\pi}{3})$$
$$+i_{kd}L_{akd}\cos(\theta - \frac{2\pi}{3}) - i_{kq}L_{akq}\sin(\theta - \frac{2\pi}{3}) \quad (3.17)$$

$$\varphi_c = -i_a[L_{ab0} + L_{aa2}\cos(2\theta - \frac{\pi}{3})] + i_b[L_{ab0} + L_{aa2}\cos(2\theta - \pi)]$$
$$-i_c[L_{aa0} + L_{aa2}\cos 2(\theta + \frac{2\pi}{3})] + i_{fd}L_{afd}\cos(\theta + \frac{2\pi}{3})$$
$$+i_{kd}L_{akd}\cos(\theta + \frac{2\pi}{3}) - i_{kq}L_{akq}\sin(\theta + \frac{2\pi}{3}) \quad (3.18)$$

3.5.2 Circuit Equation of Rotor

Voltage equation for rotor circuit defined as:

$$e_{fd} = \frac{d\varphi_{fd}}{dt} + R_{fd}i_{fd} \quad (3.19)$$

$$0 = \frac{d\varphi_{kd}}{dt} + R_{kd}i_{kd} \quad (3.20)$$

$$0 = \frac{d\varphi_{kq}}{dt} + R_{kq}i_{kq} \quad (3.21)$$

The flux linkage of rotor may be expressed as:

$$\varphi_{fd} = L_{ffd}i_{fd} + L_{fkd}i_{kd} - L_{afd}[i_a\cos\theta + i_b\cos(\theta - \frac{2\pi}{3}) + i_c\cos(\theta - \frac{2\pi}{3})] \quad (3.22)$$
$$\varphi_{kd} = L_{fkd}i_{fd} + L_{kkd}i_{kd} - L_{akd}[i_a\cos\theta + i_b\cos(\theta - \frac{2\pi}{3}) + i_c\cos(\theta + \frac{2\pi}{3})] \quad (3.23)$$

$$\varphi_{kq} = L_{kkq}i_{kq} + L_{akq}[i_a\sin\theta + i_b\sin(\theta - \frac{2\pi}{3}) + i_c\sin(\theta + \frac{2\pi}{3})] \quad (3.24)$$

3.5.3 Using Parks Transformation

Mathematical modeling of a synchronous generator is greatly simplified through variable transformation. Among these, Park's or *d-q* transformation is commonly used method to handle stator variables (currents, voltages, fluxes) (Brezovec et al., 2022). Transforming the state variables from the stationary a, b, c phase to a new frame that rotates with the rotor greatly simplifies the system's analysis. The transformed quantities are derived byprojecting the actual variables onto three axes: the direct axis, the quadrature axis, and a stationary axis.

The parks transformation notation:

$$P = \sqrt{\frac{2}{3}} \begin{bmatrix} \cos\theta & \cos(\theta - \frac{2\pi}{3}) & \cos(\theta + \frac{2\pi}{3}) \\ -\sin\theta & -\sin(\theta - \frac{2\pi}{3}) & -\sin(\theta + \frac{2\pi}{3}) \\ \sqrt{\frac{1}{2}} & \sqrt{\frac{1}{2}} & \sqrt{\frac{1}{2}} \end{bmatrix} \tag{3.25}$$

The parks transformation for current is as follow:

$$i_{dqo} = P i_{abc} \tag{3.26}$$

$$i_{dqo} = \begin{bmatrix} i_d \\ i_q \\ i_o \end{bmatrix} \qquad i_{abc} = \begin{bmatrix} i_a \\ i_b \\ i_c \end{bmatrix} \tag{3.27}$$

Due to the unique nature of Park's transformation, an inverse transformation P also exists and is defined as:

$$i_{abc} = p^{-1} i_{dqo} \tag{3.28}$$

$$P^{-1} = \sqrt{\frac{2}{3}} \begin{bmatrix} \sqrt{\frac{1}{2}} & \cos\theta & \sin\theta \\ \sqrt{\frac{1}{2}} & \cos(\theta - \frac{2\pi}{3}) & -\sin(\theta - \frac{2\pi}{3}) \\ \sqrt{\frac{1}{2}} & \cos(\theta + \frac{2\pi}{3}) & -\sin(\theta + \frac{2\pi}{3}) \end{bmatrix} \quad (3.29)$$

The parks transformation matrix is orthogonal, i.e., $P^{-1} = P^T$, signifies that it is a power-invariant transformation(Brezovec et al., 2022).

3.5.3.1 Stator flux linkage in dqo transformation

By applying parks transformation of Equation (3.25) into Equation of stator flux linkage Equation from (3.16), (3.17) and (3.18) by eliminating trigonometric terms, then we get the following expression:

$$\varphi_d = L_d i_d + L_{afd} i_{fd} + L_{akd} i_{kd} \quad (3.30)$$

$$\varphi_q = -L_q i_q + L_{akq} i_{kq} \quad (3.31)$$

$$\varphi_o = -L_o i_o \quad (3.32)$$

3.5.3.2 Rotor flux linkage in dqo components

Substituting the i_d and i_q equation into the Equation (3.22) to (3.24) gives,

$$\varphi_{fd} = L_{ffd} i_{fd} + L_{fkd} i_{kd} - \frac{3}{2} L_{afd} i_d \quad (3.33)$$

$$\varphi_{kd} = L_{fkd} i_{fd} + L_{kkd} i_{kd} - \frac{3}{2} L_{akd} i_d \quad (3.34)$$

$$\varphi_{kq} = L_{kkq} i_{kq} - \frac{3}{2} L_{akq} i_q \quad (3.35)$$

3.5.3.3 Stator voltage in dqo components

Applying the dqo transformation of Equation (3.25) yield expression for stator voltage as:

$$e_d = \frac{d\varphi_d}{dt} - \varphi_q \frac{d\theta}{dt} - R_a i_d \quad (3.36)$$

$$e_q = \frac{d\varphi_q}{dt} - \varphi_d \frac{d\theta}{dt} - R_a i_q \tag{3.37}$$

$$e_o = \frac{d\varphi_o}{dt} - R_a i_o \tag{3.38}$$

Here the θ is the angle between phase a and the d-axis, and $\frac{d\theta}{dt}$ is rotor angular velocity.

3.5.4 Electric Power and Torque

To calculate the instantaneous stator three-phase power, the following formula is used:

$$P_t = e_a i_a + e_b i_b + e_c i_c$$

Under balanced operation ($e_o = i_o = 0$), reducing phase voltage and currents in terms of dqo component yields the power as:

$$P_t = \frac{3}{2}(e_d i_d + e_q i_q) \tag{3.39}$$

The electromagnetic torque defined as:

$$T_e = \frac{3}{2}\frac{P}{2}(\varphi_d i_q + \varphi_q i_d) \tag{3.40}$$

3.5.5 Equation of Motion

3.5.5.1 Swing equation

If the torques acting on the rotor are unbalanced, the net torque responsible for acceleration (or deceleration) can be expressed as:

$$T_a = T_m - T_e \tag{3.41}$$

Where

T_a =accelerating torque in N.m

T_m =mechanical torque in N.m

T_e =electromagnetic torque in N.m

The swing equation is a differential equation that describes how any imbalance between mechanical and electromagnetic torque causes the synchronous generator and turbine (primary mover) to accelerate or decelerate:

$$J\frac{d\omega_m}{dt} = T_m - T_e \qquad (3.42)$$

Where J is combined moment of inertia in Kg.m^2, ω_m is rotor angular velocity in mech rad/s, and t is time in second.

By defining the inertia constant H as the rotor's kinetic energy in relation to the generator's base rating, one can normalize Differential Equation (3.42) to per unit (p.u.) values.

$$H = \frac{1}{2}\frac{J\omega_{om}{}^2}{S_b} \quad (3.43)$$

Where ω_{om} is the rated rotor angular velocity, in mech.rad/s. Then defining J in terms of (3.43), $J = \frac{2HS_b}{\omega_{om}{}^2}$ and substitute into Equation (3.42), obtain

$$2H\frac{d}{dt}\left(\frac{\omega_r}{\omega_o}\right) = T_m - T_e \approx P_m - P_e \qquad (3.44)$$

Where $\omega = \frac{\omega_r - \omega_o}{\omega_o}\left(=\frac{\omega_r}{\omega_o} - 1\right)$ and by substituting it into Equation (3.44), we get the per unit equation of motion as:

$$2H\frac{d\omega}{dt} = T_m - T_e \approx P_m - P_e \qquad (3.45)$$

It's often to include a component of damping torque, where D is damping coefficient and $\frac{d\delta}{dt} = \omega_r - \omega_o = \omega_o\omega$ is rotor angular velocity in electrical rad/s.

$$\frac{2H}{\omega_o}\frac{d^2\delta}{dt^2} + \frac{D}{\omega_o}\frac{d\delta}{dt} = T_m - T_e \approx P_m - P_e \qquad (3.46)$$

3.5.6 State Space Model of Synchronous Generator

Neglecting amortisseur effects offers the initial level of simplification for synchronous generator models. This approach is beneficial because it minimizes data requirements, given that relevant amortisseur machine parameters are frequently not readily accessible and also it reduces computational efforts by reducing the order of model. While higher-order models offer superior results for specific applications, their use is limited by the need for precise parameter data. However, for large systems facing data availability limitations, simpler models like (1.1) or (1.0) might be adequate, assuming their parameters are correctly established.In this thesis model (1.0) can be used which derived from above equation by considering the system performance(Ibraheem Kasim Ibraheem, 2011; KUNDUR, 1994).

As in case of classical model of generator, the swing equation are,

$$P\Delta\omega_r = \frac{1}{2\mathrm{H}}\left(T_m - T_e - K_D\Delta\omega_r\right) \tag{3.47}$$

$$P\delta = \omega_o\Delta\omega_r \tag{3.48}$$

Where

$\Delta\omega_r$ is speed deviation in p.u, $\omega_o = 2\pi f_o$ is base electrical speed of rotor in rad/s, δ is rotor angle in electrical radian.

To facilitate stability analysis in large systems, two terms are typically omitted from the stator voltage Equation (3.36) and (3.37) specifically,

- The transformer voltage terms, $P\varphi_d$ and $P\varphi_q$
- The effect of speed variation

With per unit value of $\omega_r = 1$,the stator voltage equation reduces to

$$e_d = -\varphi_q - R_a i_d \tag{3.49}$$

$$e_q = -\varphi_d - R_a i_q \tag{3.50}$$

Flux linkage reduce to

$$\varphi_d = -L_d i_d + L_{ad} i_{fd} \tag{3.51}$$

$$\varphi_q = -L_q i_q \tag{3.52}$$

$$\varphi_{fd} = -L_{ad} i_d + L_{ffd} i_{fd} \tag{3.53}$$

Rotor voltage reduce to

$$e_{fd} = P\varphi_{fd} + R_{fd} i_{fd} \tag{3.54}$$

By rearranging it

$$P\varphi_{fd} = e_{fd} - R_{fd} i_{fd} \tag{3.55}$$

The equivalent circuit related to flux linkage and current are as shown in Figure 3.4 from this flux linkage of stator and rotor are expressed by:

$$\begin{aligned}\varphi_d &= -L_l i_d + L_{ad}(-i_d + i_{fd}) \\ &= -L_l i_d + \varphi_{ad}\end{aligned} \tag{3.56}$$

$$\begin{aligned}\varphi_q &= -L_l i_q + L_{aq}(-i_q) \\ &= -L_l i_q + \varphi_{aq}\end{aligned} \tag{3.57}$$

$$\begin{aligned}\varphi_{fd} &= L_{ad}(-i_d + i_{fd}) + L_{fd} i_{fd} \\ &= \varphi_{ad} + L_{fd} i_{fd}\end{aligned} \tag{3.58}$$

In this equation φ_{ad} and φ_{aq} are the air gap flux linkage, and L_{aq} are values of the mutual inductances.

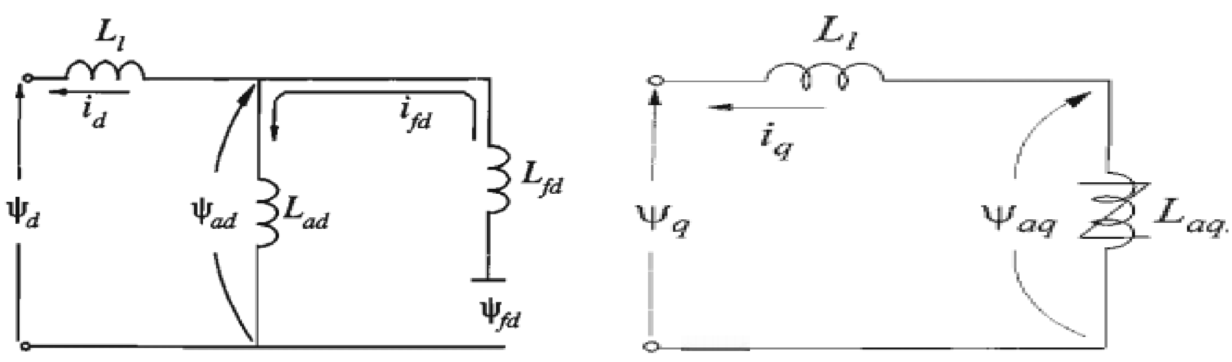

Figure 3. 4:Equivalent circuits for the direct (d) and quadrature (q) axis(KUNDUR, 1994)

From Equation (3.58), the field current defined as:

$$i_{fd} = \frac{\varphi_{fd} - \varphi_{ad}}{L_{fd}} \tag{3.59}$$

The d-axis and q-axis mutual flux linkage can write as follow

$$\begin{aligned} \varphi_{ad} &= L_{ad}'\left(-i_d + \frac{\varphi_{fd}}{L_{fd}}\right) \\ \varphi_{aq} &= -L_{aq} i_q \end{aligned} \tag{3.60}$$

And the air gap torque is

$$T_e = \varphi_{ad} i_q - \varphi_{aq} i_d \tag{3.61}$$

Linearize system equation

Express the current equation in perturbed values after expressing it in terms of δ and φ_{fd} as follow

$$\begin{aligned} \Delta i_d &= r_1 \Delta\delta + r_2 \Delta\varphi_{fd} \\ \Delta i_q &= r_3 \Delta\delta + r_4 \Delta\varphi_{fd} \end{aligned} \tag{3.62}$$

The linearized form of Equation (3.59) is as:

$$\Delta i_{fd} = \frac{1}{L_{fd}}\left(1 - \frac{L_{ad}'}{L_{fd}} + r_2 L_{ad}'\right)\Delta\varphi_{fd} + \frac{1}{L_{fd}} r_1 L_{ad}' \Delta\delta \tag{3.63}$$

Equation (3.61) can be linearized as:

$$\Delta T_e = k_1 \Delta\delta + k_2 \Delta\varphi_{fd} \tag{3.64}$$

By linearizing Equation (3.47), (3.48), (3.55) and substituting the expression for ΔT_e and Δi_{fd} given by Equation (3.63) and (3.64), we obtain the system equation in state space form as bellow

$$\begin{bmatrix} P\Delta\omega_r \\ P\Delta\delta \\ P\Delta\varphi_{fd} \end{bmatrix} = \begin{bmatrix} a_{11} & a_{12} & a_{13} \\ a_{21} & 0 & 0 \\ 0 & a_{32} & a_{33} \end{bmatrix} \begin{bmatrix} \Delta\omega_r \\ \Delta\delta \\ \Delta\varphi_{fd} \end{bmatrix} + \begin{bmatrix} b_{11} & 0 \\ 0 & 0 \\ 0 & b_{32} \end{bmatrix} \begin{bmatrix} \Delta T_m \\ \Delta E_{fd} \end{bmatrix} \tag{3.65}$$

3.6 Modeling of Excitation/AVR

In synchronous generator AVR system can be employ to maintain the magnitude of the terminal voltage at a given level. During typical, slight, and gradual variations in the load, the alternator terminal voltage must remain constant. The main component used to design AVR system include Amplifier, Exciters, Generator and Sensor(Ezenugu & Nwokonko, 2024).The mathematical model and transfer functions can be linear considering the time constant and gain by ignoring saturation or other nonlinear except for generator model. Since the loops operate near a normal state with only small variations, they can be precisely described by linear transfer functions and modeled using linear, constant-coefficient differential equations. The comparator compares generate an error voltage (V_e) or error signal by comparing the measured signal voltage against the reference voltage (Mosaad et al., 2019). The Comparator Modeling is, the error signal $V_e = V_{ref} - V_t$ the Laplace transformation of this equation is:

$$|V_e(s)| = |V_{ref}(s)| - |V_t(s)| \tag{3.66}$$

3.6.1 Amplifier Model

Continuously monitoring the reference voltage (V_{ref}) against the actual output voltage (V_t), thecomparator generates a voltage error signal that feeds into the amplifier. The excitation system amplifier could be a magnetic amplifier, rotating amplifier, or modern electronic amplifier(Hadi Saadat, 1999). First order transfer function of an amplifier is modelled using gain and time constant given by:

$$V_A = K_A V_e \tag{3.67}$$

Laplace transformation given as:

$$V_A(s) = K_A V_e(s) \tag{3.68}$$

While this equation suggests instantaneous amplifier response, real world amplifier will have a time delay, modeled by time constant Ta. Then $V_A(s)$and V_e(s) are related as:

$$V_A(s) = \frac{K_A}{1 + sT_A} V_e(s) \tag{3.69}$$

The transfer function of amplifier is defined as:

$$G_A(s) = \frac{V_A(s)}{V_e(s)} = \frac{K_A}{1+sT_A} \tag{3.70}$$

Where V_A is amplifier output voltage, V_e is Voltage error, K_A is amplifier gain and, T_A is amplifier time constant. The block diagram representing equations of comparator and amplifier is shown in Figure 3.5.

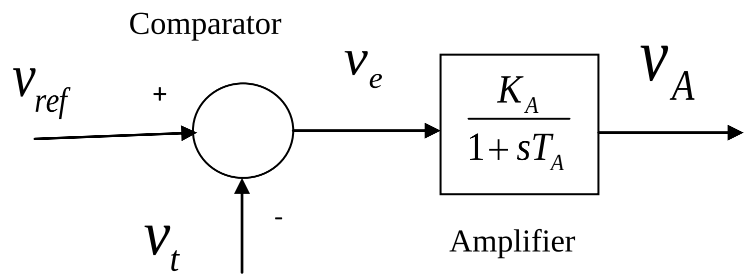

Figure 3. 5:Amplifier block diagram(Hadi Saadat, 1999)

3.6.2 Exciter Modeling

An exciter, which can be a static device or another machine, provides the excitation for the alternators. The primary part of the AVR loop is the exciter. It provides the alternator field with DC power.A linearized model is a fair representation of a modern exciter since it considers the primary time constant while disregarding saturation or other nonlinearities(Hadi Saadat, 1999). The exciter takes the amplified error signal from the amplifier and excites the alternator field to control flux and hence controls the terminal voltage(KUNDUR, 1994). Note that $V_e = |V_{ref}| - |V_t|$ is error voltage. Assume that the primary generator's terminal voltage drops for any cause. This will result in decrease in the terminal voltage |V|. immediately this raises the "error voltage" V_e which leads to increased values of V_A, i_e and V_f The raise of V_{ref} also will have the same effect of increasing the terminal voltage. The modeling of the exciter field is as follows.

$$E_{fd} = \frac{d\varphi_{fd}}{dt} + R_{fd} i_{fd} \tag{3.71}$$

The field current i_{fd} of exciter generate voltage E_{fd} of exciter rectified armature voltage. Then we get:

$$\Delta E_{fd} = K_1 \Delta i_{fd} \tag{3.72}$$

By applying Laplace transformation to the above two equations and eliminating $\Delta i_{fd}(s)$, a modern exciter transfer function can be represented by time constant T_E and a gain K_E

$$G_E(s) = \frac{E_{fd}(s)}{V_A(s)} = \frac{K_E}{1+sT_E} \tag{3.73}$$

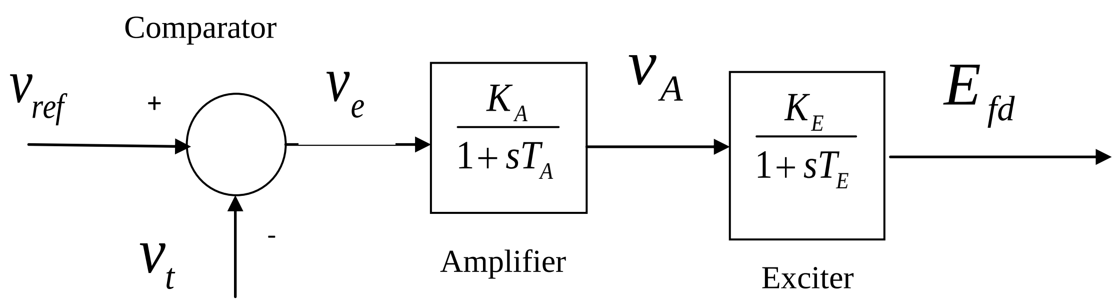

Figure 3. 6:Exciter and Amplifier block diagram

Open loop transfer function representation of amplifier and exciter shown in Figure 3.6 is:

$$\begin{aligned} G_{ex}(s) &= G_A(s) * G_E(s) \\ &= \frac{K_A K_E}{(1+sT_A)(1+sT_E)} \end{aligned} \tag{3.74}$$

Where K_A and K_E is amplifier gain and exciter gain respectively, and T_A and T_E represent the time constant.

3.6.3 Sensor Model

The sensor used for feedback loop in this system is voltage transducer, primary sensor that detects terminal voltage of the generators. The voltage transducer is described by first order transfer function, is given by:

$$\frac{\Delta V_t}{\Delta E_t} = \frac{1}{1+sT_R} \tag{3.75}$$

where ΔV_t is sensor output voltage and T_R is sensor time constant its value is varying in the range of (0.001 to 0.06).

3.7 Plant Model without Controller

For the excitation system, the generator terminal voltage E_t is standard input control signal and it needs to be expressed in terms of the state variable $\Delta\omega_r$, $\Delta\delta$ and $\Delta\varphi_{fd}$.This generator terminal voltage expressed as:

$$E_t^{\ 2} = e_d^{\ 2} + e_q^{\ 2} \tag{3.76}$$

After applying a small perturbation and linearizing Equation (3.77) it become

$$\Delta E_t = K_5 \Delta\delta + K_6 \Delta\varphi_{fd} \tag{3.77}$$

Here we used output terminal voltage as state variable since its feedback through voltage transducer and we have second order model for the AVR(amplifier and exciter), the order of overall plant system is increased by 3,the new state variable added is ΔV_t ,ΔV_A and ΔE_{fd} .

From sensor (voltage transducer) block of Figure 3.7, and using perturbed value, we have

$$\Delta V_t = \frac{1}{1+sT_R} \Delta E_t \tag{3.78}$$

Hence

$$P\Delta V_t = \frac{1}{T_R}\left(\Delta E_t - \Delta V_t\right) \tag{3.79}$$

By substituting for ΔE_t from Equation (3.78), we get

$$P\Delta V_t = \frac{K_5}{T_R}\Delta\delta + \frac{K_6}{T_R}\Delta\varphi_{fd} - \frac{1}{T_R}\Delta V_t \tag{3.80}$$

This paper presents a simplified block diagram model of a synchronous generator using the d-q axis approach. It includes the field winding dynamics along the d-axis but ignores the effects of damper windings, making the model more manageable for controller design and analysis.The plant system's block diagram is shown in Figure 3.7. In this representation the dynamic characteristics of the system are expressed in terms of the so-called K constant(KUNDUR, 1994).

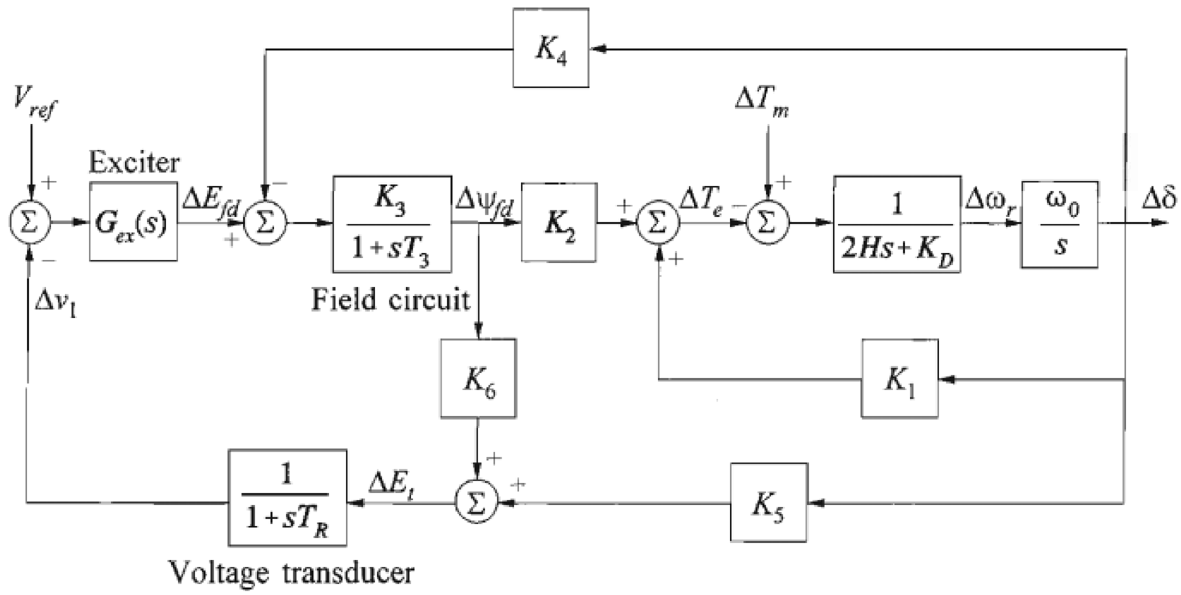

Figure 3. 7:Block diagram representation of plant without controller(KUNDUR, 1994)

State space representation of the block diagram expressed as:

$$\dot{x} = Ax + Bu$$
$$y = Cx + Du \qquad (3.81)$$

<u>Let</u>

$x_1 = \Delta\omega_r$, $x_2 = \Delta\delta$, $x_3 = \Delta\varphi_{fd}$, $x_4 = \Delta V_t$, $x_5 = \Delta V_A(s)$ and $x_6 = \Delta E_{fd}(s)$

$$\begin{bmatrix} \dot{x}_1 \\ \dot{x}_2 \\ \dot{x}_3 \\ \dot{x}_4 \\ \dot{x}_5 \\ \dot{x}_6 \end{bmatrix} = \begin{bmatrix} -\frac{K_D}{2H} & -\frac{K_1}{2H} & -\frac{K_2}{2H} & 0 & 0 & 0 \\ \omega_o & 0 & 0 & 0 & 0 & 0 \\ 0 & -\frac{K_3K_4}{T_3} & -\frac{1}{T_3} & 0 & 0 & \frac{K_3}{T_3} \\ 0 & \frac{K_5}{T_R} & \frac{K_6}{T_R} & -\frac{1}{T_R} & 0 & 0 \\ 0 & 0 & 0 & 0 & -\frac{1}{T_A} & 0 \\ 0 & 0 & 0 & 0 & \frac{K_E}{T_E} & -\frac{1}{T_E} \end{bmatrix} \begin{bmatrix} x_1 \\ x_2 \\ x_3 \\ x_4 \\ x_5 \\ x_6 \end{bmatrix} + \begin{bmatrix} 0 & \frac{1}{2H} \\ 0 & 0 \\ 0 & 0 \\ 0 & 0 \\ \frac{K_A}{T_A} & 0 \\ 0 & 0 \end{bmatrix} \begin{bmatrix} Vref & \Delta T_m \end{bmatrix}$$

$$y = \begin{bmatrix} 0 & 0 & 0 & 1 & 0 & 0 \end{bmatrix} \begin{bmatrix} x_1 \\ x_2 \\ x_3 \\ x_4 \\ x_5 \\ x_6 \end{bmatrix} \tag{3.82}$$

The following standard parameter value of synchronous generator used to calculate the Heffron-Phillips constant(K1-K6) that employed in my state space representation.

Table 3. 1:Standard parameter value of synchronous generator(KUNDUR, 1994)

Standard Parameter	Description	Value	Unit
S	rated power	555	MVA
V	Rated voltage	24	KV
Pf	Power factor	0.9	P.u
f	Rated frequency	60	Hz
ω_r	Rotor speed	3600	RPM
R_a	Armature resistance per phase	0.003	P.u
X_d	d-axis synchronous reactance	1.81	P.u
X_q	q-axis synchronous reactance	1.76	P.u

X_l	Stator linkage reactance	0.15	P.u
$X_d^{'}$	d-axis transient reactance	0.3	P.u
$T_{d0}^{'}$	d-axis OC time constant	8.0	Sec

CHAPTER FOUR

4.CONTROLLER DESIGN

4.1Theory of Fractional Calculus

The field of mathematics known as Fractional Order Calculus (FOC) deals with differentiation and integration under any real or complex number. One major advantage is the improved controllability of dynamic systems that are mathematically described by fractional orders. Furthermore, the $PI^{\lambda}D^{\mu}$ controller demonstrate greater robustness against changes in system and controller parameters(Podlubny, 1999). Fractional calculus is the extension of integration and differentiation to non-integral order integro-differential operatorsD_t^{α} , where a and t are the lower and upper limits and a $\alpha(\alpha \in R)$ is the order of the operation. The continuous integro-differential operator is defined as(Ramezanian et al., 2013).

$$ {}_aD_t^{\alpha} = \begin{cases} \dfrac{d^{\alpha}}{dt^{\alpha}} & R(\alpha) > 0, \\ 1 & R(\alpha) = 0, \\ \int_a^t (d\tau)^{-\alpha} & R(\alpha) < 0 \end{cases} \qquad (4.1) $$

<u>where</u>

a and t are limit of operation

α-fractional order $\alpha \in R$

According to (Li et al., 2017) fractional derivatives and integrals are commonly defined in the time-domain by the Grünwald-Letnikov (GL), Riemann–Liouville (RL), and Caputo (C) definitions, which are given as:

A. Definition of Grünwald-Letnikov (GL)

$$ {}_aD_t^{\alpha} f(t) = \lim_{h \to 0} h^{-\alpha} \sum_{j=0}^{\left[\frac{t-a}{h}\right]} (-1)^j \binom{\alpha}{j} f(t - jh) \qquad (4.2) $$

Where h is a grid size, $[.]$means the part of integral, and $\binom{\alpha}{j}$is a binomial coefficient.

B. Definition of Riemann–Liouville (RL)

$$ {}_{a}D_{t}^{\alpha} f(t) = \frac{1}{\Gamma(m-a)} \left(\frac{d}{dt}\right)^{m} \int_{a}^{t} \frac{f(\tau)}{(t-\tau)^{\alpha-m+1}} d\tau \tag{4.3} $$

Where$\Gamma(\ .)$ is the Euler Gamma function and m-1 $<\alpha < m$, m$\in N$

C. Definition of Caputo (C)

$$ {}_{0}D_{t}^{\alpha} f(t) = \frac{1}{\Gamma(m-a)} \int_{0}^{t} \frac{f^{(m)}(\tau)}{(t-\tau)^{\alpha-m+1}} d\tau \tag{4.4} $$

Where

m-1 $<\alpha < m$, m$\in N$

Engineers commonly use the Laplace transform method. The Laplace transform for the RL fractional derivative in Equation (4.3) is expressed as:

$$ \int_{0}^{\infty} e^{-st} {}_{0}D^{\alpha}{}_{t} f(t) dt = s^{\alpha} F(s) - \sum_{k=0}^{m-1} s^{k} {}_{0}D_{t}^{\alpha-k-1} f(t) |_{t=0} \tag{4.5} $$

For $(m-1 < \alpha \leq m)$,where s ≡ jω denotes the Laplace transform variable

4.2 Oustaloup's Approximation Algorithm

While numerical solutions for fractional differential equations are essential in practice, directly implementing time-domain fractional operators is challenging. To address this challenge, approximation methods were adopted. The fundamental approach is to estimate fractional operators by using standard integer order counterparts(Li et al., 2017).FOMCON relies heavily on approximations of fractional order systems, and Oustaloup's recursive filter approximation is typically employed, while alternative techniques are also available. Oustaloup's approach represents a band limited approximation of a fractional-order operator using standard transfer functions.The following equations are used to calculate fractional integrator of order (−α) or fractional differentiator of order α in order to approximate them by a standard transfer function.(Tepljakov et al., 2019).

$$ s^{\alpha} \approx K \prod_{K=1}^{N} \frac{s + w_{k}'}{s + w_{k}} \tag{4.6} $$

where the poles, zeros, and gain of the filter can be calculated from:

$$w_k' = w_b \left(\sqrt{\frac{w_h}{w_b}} \right)^{(2k-1-\alpha)/N}$$
$$w_k = w_b \left(\sqrt{\frac{w_h}{w_b}} \right)^{(2k-1+\alpha)/N} \tag{4.7}$$
$$K = w_h^{\alpha}$$

Nis the order of approximation in the valid frequency range ($w_b ; w_h$).In this thesis, fifth-order Oustaloup's approximation algorithm is used to approximate the transfer function of fractional order within a frequency range of $\omega \in (10^{-2} - 10^{+2})$ rad/s .

4.3 Fractional Order PID Controller Design

Due to having two extra parameters that is an integrator of order λand differentiator of order μ**,**Podlubnyproposed a generalization of the PID-controller, known as FOPID thatperforms better than the conventional PID-controller when used to control fractional-order systems.

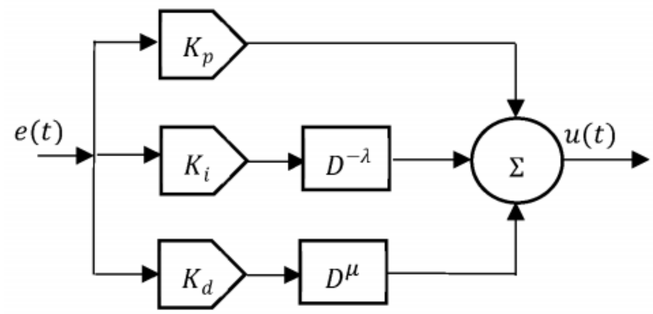

Figure 4. 1:Block diagram of a fractional-order PID (FOPID) controller(Podlubny, 1999)

A FOPID controller is defined by five parameters: proportional, integral, and differential gains, along with integral and differential orders. The transfer function of such the $PI^{\lambda}D^{\mu}$-controller has the form:

$$G_C(s) = K_p + K_i s^{-\lambda} + K_d s^{\mu} \tag{4.8}$$

Conventional controllers, including PID, PI, PD, and purely proportional(P) controllers, can be seen as special cases derived from a more general FOPID controller.By appropriately adjusting the parameters λ and μ within the FOPID structure, it is possible to replace these simpler controller types. Specifically,a conventional PID controller is achieved whenλand μ are both set to 1(Li et al., 2017).

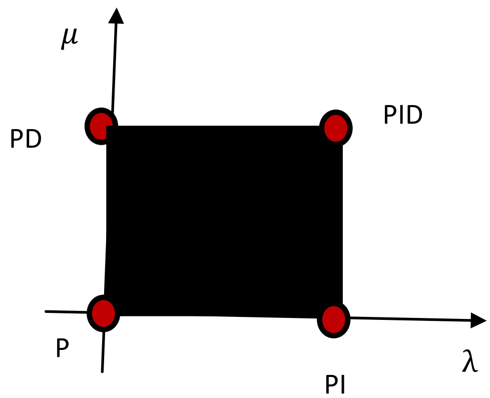

Figure 4. 2:Realization of PID controllers with FOPID controller(Verma et al., 2017)

Time domain transfer function of FOPID controllers defined as:

$$u(t) = K_p e(t) + K_i D^{-\lambda} e(t) + K_d D^{\mu} e(t) \tag{4.9}$$

In this equation, u(t) indicate control variable, while e(t) is error signal in time domain given as**:**

$$e(t) = V_{ref}(t) - V_t(t) \tag{4.10}$$

Where $V_t(t)$ is output terminal voltage of synchronous generator.

The proportional term (K_p) Provides immediate control action proportional to the current error, used to improve response speed. The integral term (K_i) Eliminates steady-state errors by adding previous errors and driving the system to the desired setpoint. The fractional order **λ** allows for more control over the rate of error accumulation. While the Derivative term (K_d)predicate future errors based on the rate of change of the error, that used for improving damping and reducing overshoot. The fractional order μ more versatile in shaping the derivative action, enhancing transient response and noise filtering compared to a standard differentiator (μ = 1).

4.4PID ControllerDesign for Performance Comparison

One of the widely used feedback control mechanism is PID controllers. In this thesis, it serves as a benchmark for comparative analysis against the proposed FOPID controller, allowing for a clear evaluation of the FOPID controller's performance enhancements in synchronous generator voltage regulation. It consists of three components which are proportional term (K_p), the integral term (K_i) and the derivative term (K_d). A heuristic approach to PID controller tuning is the Ziegler-Nichols tuning method. The process is carried out by setting the derivative (D) and integral (I) gains to zero. After that, the P (proportional) gain is raised from zero to the ultimate gain, where the closed loop's output exhibits steady and reliable oscillations. The idea behind relay auto-tuning is the observation that the system may oscillate with the period T_u under relay control(Ellis, 2012; Hang et al., 2002). As depicted in Figure 4.3, the system is placed in a feedback loop to calculate the critical point. The output y(t) is a periodic signal with the period T_u and the ultimate gain K_u is roughly described by the relay description function being in the negative real axis:

$$K_u = \frac{4d}{\pi a} \tag{4.11}$$

Where d is relay amplitude and a is amplitude of system output.

Using system critical point, Z-N tuning rule can be used to optimize the PID controllers, the PID setting are given by:

$$\begin{aligned} K_p &= \frac{K_u}{1.7} \\ T_i &= \frac{T_u}{2} \\ T_d &= \frac{T_u}{8} \end{aligned} \tag{4.12}$$

Where $K_i = \frac{K_p}{T_i}$ and $K_d = K_p T_d$

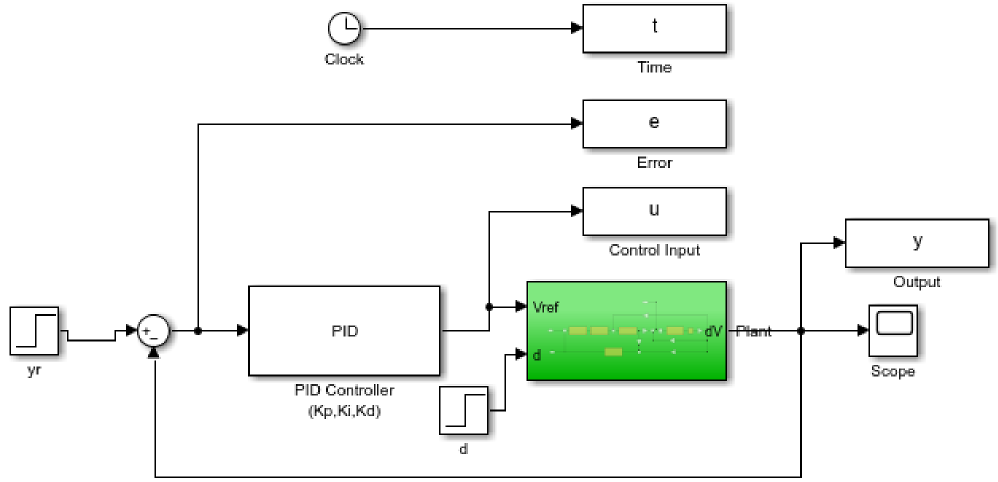

Figure 4. 3:Simulink representation of the closed-loop system with a PID controller

4.5 GWO-Based FOPID Controller Parameter Optimization

To determine the optimal values for the FOPID controller parameters, optimization of controller parameters is crucial. Over the past 20 years, meta-heuristic optimization techniques have gained a lot of popularity. This thesis employs GWO to adjust the parameters of FOPID controller since GWO provides an effective balance between exploration and exploitation and making it well-suited for tuning FOPID controller parameters to achieve desired voltage regulation performance. As shown in Figure 4.4, the dominating behavior of the grey wolves determines their social hierarchy. Alpha (α) represents the top level, which is the most dominant level in the hierarchy. Beta (β), which aids α in the hunting phase, shares the second rung of the hierarchy. As a subordinate, the delta (δ) wolf represents the third level. The omega (ω) wolves constitute the final hierarchical level, serving as the group's followers(Mirjalili et al., 2014).

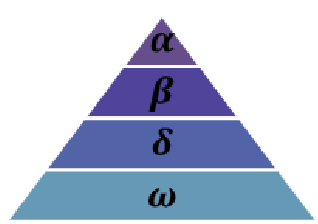

Figure 4. 4:Hierarchical Structure of Grey Wolves(Mirjalili et al., 2014)

The GWO algorithm is being followed by the following steps:

A. Search for Prey

The grey wolf uses the positions of alpha, beta, and delta to find its prey. As a result, the search process takes different routes, demonstrating the GWO technique's exploratory character.

B. Encircling the Prey

The encircling behavior described by following equations

$$\vec{D} = |\vec{C}\,\vec{X}_P(t) - \vec{X}(t)| \tag{4.13}$$

$$\vec{X}(t+1) = \vec{X}_p(t) - \vec{A}.\vec{D} \tag{4.14}$$

where t indicates the current iteration, $\vec{A}$ and $\vec{C}$ are coefficient vectors, $\vec{X}_p$ is the position vector of the prey, and $\vec{X}$ indicates the position vector of a grey wolf. The vectors $\vec{A}$ and $\vec{C}$ are calculated as follows:

$$\vec{A} = 2a.r_1 - a \tag{4.15}$$

$$\vec{C} = 2.r_2 \tag{4.16}$$

where ‘a’ linearly decreased from 2 to 0 over the course of iterations and r1, r2 are random vectors in [0,1].

C. Hunting Behaviors

Grey wolves are capable of locating their prey and encircling them. The alpha typically leads the hunt. On occasion, the beta and delta may also engage in hunting. The wolf positions are updated as follow:

$$\begin{aligned} \vec{D}_{\alpha i} &= |C_1.\vec{X}_{\alpha i}(t) - \vec{X}_i(t)| \\ \vec{D}_{\beta i} &= |C_2.\vec{X}_{\beta i}(t) - \vec{X}_i(t)| \\ \vec{D}_{\delta i} &= |C_3.\vec{X}_{\delta i}(t) - \vec{X}_i(t)| \end{aligned} \tag{4.17}$$

$$\vec{X}_{i1} = \vec{X}_{\alpha i}(t) - A_1 . \vec{D}_{\alpha i}$$
$$\vec{X}_{i2} = \vec{X}_{\beta i}(t) - A_2 . \vec{D}_{\beta i} \tag{4.18}$$
$$\vec{X}_{i3} = \vec{X}_{\delta i}(t) - A_3 . \vec{D}_{\delta i}$$

$$\vec{X}_i(t+1) = \frac{\vec{X}_{i1} + \vec{X}_{i2} + \vec{X}_{i3}}{3} \tag{4.19}$$

where $\vec{X}_i(t+1)$ is the best search agent for iteration i.

D. Attacking Prey(exploitation)

Decreasing the coefficient vector, A brings the grey wolves closer to the prey. Thus, to lower A, the value of 'a' must be minimized, as follows:

$$a = 2 - \left(\frac{2}{\max .iteriation} \right) \tag{4.20}$$

where a linearly decreases from 2 to 0 over iterations.

In this paper, in order to optimize the parameters of FOPID controller, the range values of K_p, K_i, K_d, λ and μ are selected from manual tuning method based on stability criteria. Integral absolute error (IAE) used as an objective function because IAE measure the total absolute value of the error signal over time, offering a straightforward indication of overall system tracking performance by equally weighting errors across the entire response period. The cost function J is chosen based on performance criteria given as:

$$J = \int_0^{\infty} | e(t) | dt \tag{4.21}$$

The error signal, e(t)**,** is calculated as the difference between the reference voltage (set-point) and the synchronous generator's terminal voltage**,** where tis the simulation time**.**Different performance metrics parameters like rising time, settling time, peak time, and overshoot are used to assess the performance of synchronous generator voltage regulation. These parameters evaluate the controller effectiveness to regulates the output voltage of the system. The main goal of this algorithm's is to find the parameter set that results in the smallest possible value of this integral, which achieve the desired voltage regulation performance with minimal error over time, especially penalizing errors that persist. the mathematical expression of this optimization problem has defined below.

Objective Function:

$$F_1 = \min \left| \int_0^{\infty} |e(t)|\, dt \right| \tag{4.22}$$

Subjected to Parameter constraints:

$$\begin{aligned} &K_p^{\min} \le K_p \le K_p^{\max} \\ &K_i^{\min} \le K_i \le K_i^{\max} \\ &K_d^{\min} \le K_d \le K_d^{\max} \\ &\lambda^{\min} \le \lambda \le \lambda^{\max} \\ &\mu^{\min} \le \mu \le \mu^{\max} \end{aligned} \tag{4.23}$$

Input Saturation constraints

The saturation limit block in an AVR is used to prevent excessive excitation voltage that could damage the generator's field winding or lead to instability in the system. It ensures that the field voltage remains within safe operational limits. The control signal u(t) is constrained by a saturation function which limits the controller output to be within the physical bounds to prevent over driving the excitation system. The control signal used for the plant is therefore U_{sat} (t).

$$U_{sat} = \begin{cases} U_{\max}, U > U_{\max} \\ U_{\min}, U < U_{\min} \\ U, otherwise \end{cases} \tag{4.24}$$

<u>Where</u>

U_{sat} is saturated output

U_{max} is maximum allowable value and,

U_{min} is minimum allowable value

An AVR system, which typically comprises of four parts, an amplifier, exciter, generator, and sensor, is installed in an excitation system to maintain the terminal voltage magnitude of a synchronous generator at a predetermined level. In Chapter 3 the open loop state space of the plant including all these four AVR component can be modeled so now we connect the FOPID controller with unity feedback to form closed loop system model. The AVR system adapted with a FOPID controller is shown in Figure 4.5.

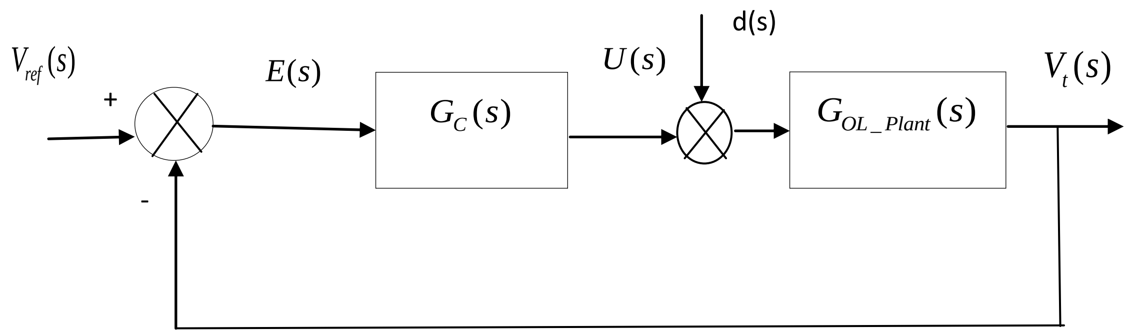

Figure 4. 5: Integration of a FOPID Controller into an AVR System Block Diagram(Micev et al., 2020)

CHAPTER FIVE

5. RESULT AND DISCUSSION

5.1 Chapter Overview

This chapter presents and analyzes the results obtained from the implementation and simulation of the GWO based FOPID controller for the AVR system, including a detailed analysis of its performance and robustness. The simulations were conducted using the MATLAB/Simulink environment, a powerful platform for modeling and simulating dynamic systems. This allowed for a comprehensive assessment of the proposed GWO-FOPID controller's performance compared to PID controller.The overall proposed control system Simulink block diagram is shown in Figure 5.1.

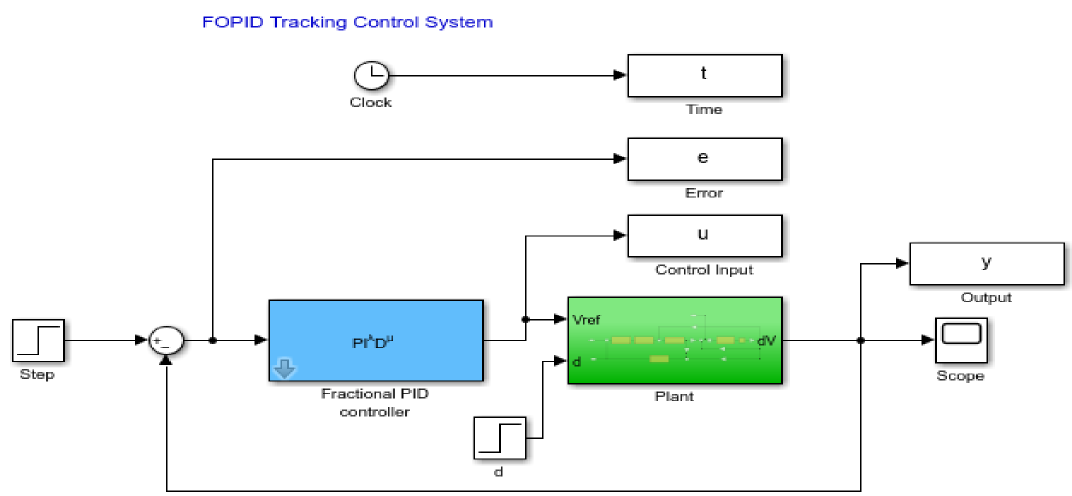

Figure 5. 1:Simulink diagram of proposed system

5.2 AVR of Synchronous Generator and Controller Parameter

5.2.1Parameter of AVR of Synchronous Generator

The parameters of the AVR component used in simulation are listed in Table 5.1(Hadi Saadat, 1999), and also the parameter of the Heffron-Phillips constant(K1-K6) can be derived from the standard parameter of the synchronous generator listed in Chapter three Table 3.1.

Table 5. 1:The parameter value of AVR used in the simulation(Hadi Saadat, 1999)

Parameter	Description	Value	Unit
K_A	Amplifier gain	50	p.u
T_A	Amplifier time constant	0.1	Sec
K_E	Exciter gain	1	p.u
T_E	Exciter time constant	0.4	Sec
T_R	Sensor time constant	0.05	Sec
K_1	Synchronous machine factor	1.820	p.u
K_2	>>	1.269	p.u
K_3	>>	0.230	p.u
K_4	>>	2.659	p.u
K_5	>>	0.018	p.u
K_6	>>	0.169	p.u
T_3	Field circuit time constant	1.675	Sec
H	Inertia constant	3.5	MW s/MVA
K_D	Damping coefficient	0.5	p.u

The continuous-time state space representation of the linearized open-loop plant model is expressed in Equation (3.82) then by substituting the values of the AVR of synchronous generator parameters given in Table 5.1, we can further transform to transfer function model as:

$$G_{OL\_Plant}(s) = \frac{578.8s^2 + 41.33s + 5.253\times10^4}{s^6 + 33.17s^5 + 394.8s^4 + 3904s^3 + 2.839\times10^4 s^2 + 5.827\times10^4 s + 1.681\times10^4} \quad (5.1)$$

5.2.2 Controller Parameter Setting

5.2.2.1 FOPID Controller

The FOPID controller have five parameters named as K_p, K_i, K_d, λ and μ.The grey wolf optimization is used to tune this parameter to get better tracking performance (Mirjalili et al., 2014). The GWO parameter used in the simulation are listed in the Table 5.2.

Table 5. 2:Parameter setting of GWO optimization(Mirjalili et al., 2014)

Parameters	**Value**	
Search agent	40	
Maximum Iteration	30	
Number of the parameter	5	
	Lower bound	**Upper bound**
K_p	0	5
K_i	0	5
K_d	0	5
λ	0	2
μ	0	2

Due to the inherent randomness of the optimization algorithm at its initialization, the proposed objective function (Equation 4.21) was evaluated across 30 simulation runs using the parameters detailed in Table 5.2. To manage excessive control action and enhance overall system performance control effort penalty, weighted at 0.1, was integrated into the Integral Absolute Error (IAE) performance index. This adjustment aimed to find a balance between accurate tracking (minimized by IAE) and the operational constraints of the AVR system's exciters. Given that input saturation led to system instability, this control effort penalty was used as an alternative to maintain the input within a safe operating range, thus preventing potential damage to the AVR exciter. The most favorable outcome of the GWO techniques, including the control effort, is graphically show in Figure 5.2, having a minimum function value of 2.5963 achieved at the 12th iteration. In contrast, when the simulation was run for 30 iteration focusing solely on minimizing the IAE (without the control effort penalty), a lower minimum fitness value of 0.5072 was obtained. Despite this increase in the best fitness value, including the penalty term offers potential benefits such as improved energy efficiency, reduce wear and tear on exciter or actuator, and decreased sensitivity to disturbance associated with excessive control effort.

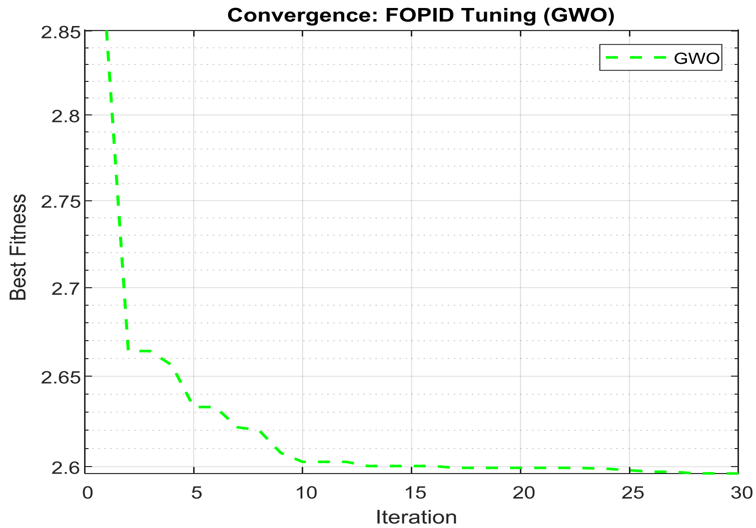

Figure 5. 2:Convergence curve of the GWO algorithm

The GWO optimized parameter values of the proposed FOPID are shown in Table 5.3.

Table 5. 3:Tuned FOPID Controller Best Parameter

Parameters	K_p	K_i	K_d	λ	μ
GWO-tuned value	1.1067	4.4283	1.8843	1.764	0.66017

5.2.2.2 PID Controller Parameter Tuning

By assuming the magnitude of switching signal applied by the relay d=1, and calculating the amplitude of the oscillation observed at the controlled variables as shown in Figure 5.3, get the value of a=0.172 and by measuring the time between two consecutive peaks in the controlled variable oscillation(Tu=1.5312) and also using Equation (4.11) the value of ultimate gain, Ku is calculated as 7.4063.The Simulink block diagram of this feedback relay tuning method used for calculating the optimal parameters of PID is depicted in appendix.

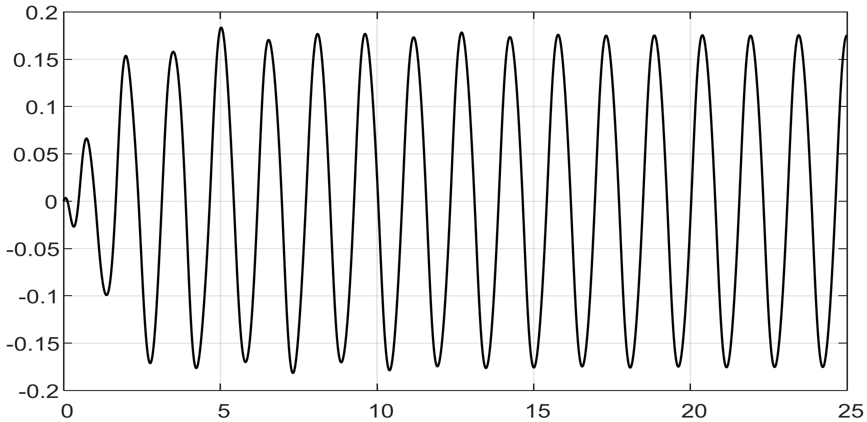

Figure 5. 3:Feedback relay tuning of PID controller

By using the Z-N tuning formula described in Equation (4.12), I calculate the best PID parameters value as shown in table.

Table 5. 4:Best Z-N tuned parameters

Parameters	K_p	K_i	K_d
Z-N tuned value	4.3544	5.6876	0.8334

5.3 Simulation Result

In this subsection, the dynamic response or tracking performance evaluation is carried out. AVR system is simulated for single step reference voltage under normal conditions, that is, without external disturbance and load variation.

5.3.1Open-Loop Performance Test

The open-loop step response of the system is depicted in Figure 5.4. The result shows a slow and sluggish rise towards the steady-state value, taking 11.987 seconds to settle. While the open-loop response showing no overshoot, the final output of the terminal voltage (Vt) settles significantly far from the desired reference input, indicating a substantial steady state error value of 2.1255. As shown in Figure 5.4 the open loop system has slow response and unable to track the reference signal accurately.

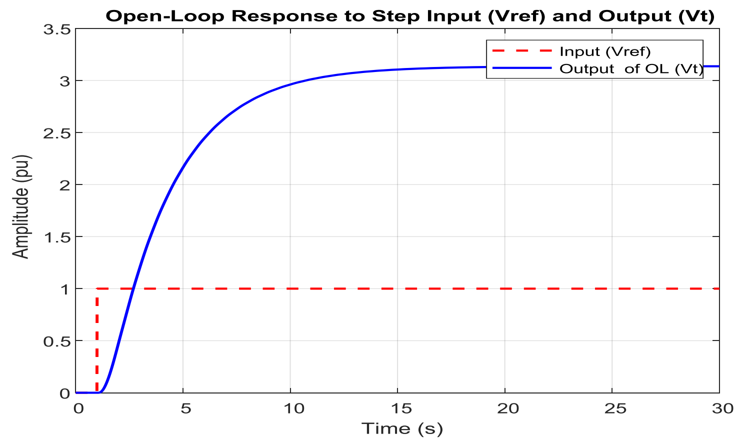

Figure 5. 4:Open-loop Response of AVR system

5.3.2 Performance Tracking of AVR using GWO tuned FOPID controller

The closed-loop step response with the proposed system demonstrates significantly improved performance compared to the open-loop system. There is a short rise time of 0.4447 seconds that indicates a fast response to the input reference. There is also an insignificant overshoot of 11.39% and the output settles quickly within 3.54 seconds, showing that have good damping. The peak value reaches 1.1140, and it occurs very early at 0.9280 seconds. The use of the IAE objective function with a control effort penalty (IAEU = 2.5963) has resulted in a balanced performance, achieving good tracking while likely limiting excessive control action u, as shown in Figure 5.5. The oscillations in the control signal are relatively small and quickly diminish.

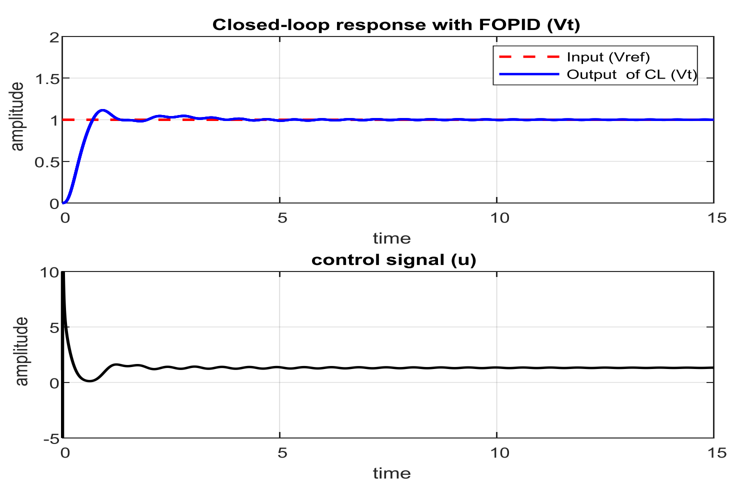

Figure 5. 5:Closed-loop response with proposed controller

5.3.3 Performance Tracking of AVR PID controller

This simulation is used for comparison purpose of conventional PID controller with the proposed GWO based FOPID controller. The PID controller is tuned using feedback relay to get value of Ku and Tu that used to calculate the optimal value of its parameter based on Z-N tuning method.The closed-loop step response with PID controller shows a fast rise time of 0.4056 seconds but it has high overshoot, reaching 46.676% with a peak value of 1.4608 at 1.1 seconds. The settling time of 4.1445 seconds is also longer compared to that of FOPID controller. The higher IAEU value of 2.9865, considering the control effort, indicates less efficient control action in achieving the desired tracking. The oscillations in both the output and the control signal, as depicted in Figure 5.6, a less damped response compared to the proposed GWO-optimized FOPID controller, highlighting the superior performance of the proposed system in terms of reduced overshoot, faster settling, and more efficient control effort.

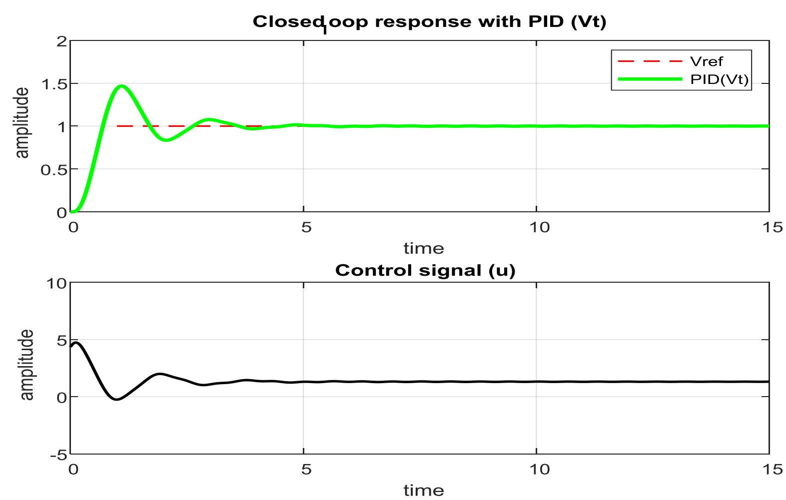

Figure 5. 6:Closed-loop response with Z-N PID controller

Table 5.5 quantitatively compares the open-loop, PID and FOPID control strategies using the key performance metrics, including rise time, settling time, minimum overshoot, peak time and the IAE with control effort penalty (IAEU). In the table below the bolded values indicate superior performance. As we can see from the Table 5.5 the proposed system demonstrates better overall performance than the Z-N tuned PID controller, which exhibits a less damped response and a higher IAEU value. While the PID controller shows slightly faster rise time, the proposed system achieves significantly improved tracking performance. Additionally, when compared to the open-loop response, the proposed system gives high improvement in both transient and steady state characteristics. Figure 5.7 shows the step response of terminal voltage and control signal for the closed-loop response of PID and FOPID controller proposed system.

Table 5. 5:Performance Comparison Table Under Normal Condition

Controller	Performance Metrics				
	Maximum overshoot	Rise time	Settling time	Peak time	IAEU
FOPID	11.397	0.4447	**3.5410**	**0.9280**	**2.5963**
PID	46.676	**0.4056**	4.1445	1.100	2.9865

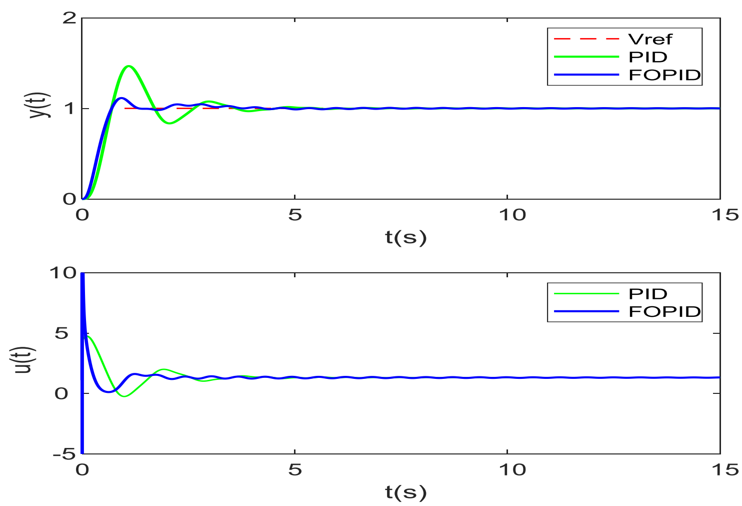

Figure 5. 7:Comparison plot of Closed-loop response with its control signal

5.4 Robustness Tracking Test

In this subsection, we consider three scenarios to test the robustness of the proposed controllers. The first scenario is parameters uncertainty test followed by the second scenario by changing reference input and finally the robustness was tested by adding external disturbance delta Tm to the plant system.

5.4.1 Performance Tracking Test to Parameters Uncertainty

To check the robustness of the proposed FOPID controller compared to that of PID controller, simulations were conducted under parameter uncertainty by varying the amplifier gain KA in the

AVR system. Here we consider two test cases. Case one, the amplifier gain was increased by 50% from its original value of 50 p.u. to 75 p.u., and in the second case, it decreased by 50% to 25 p.u. These variations simulate real-world uncertainties such as component aging or gain drift in the control circuit.

Case1: Increased Amplifier Gain (+50%)

In this case the amplifier gain was increased by 50%, both controllers experienced changes in their system dynamic performance. The FOPID controller responded faster but with a slight increase in overshoot and settling time, indicating a trade-off between speed and stability when compared with nominal value of amplifier gain. The simulation result as we can see from Figure 5.10 demonstrate that the proposed FOPID controller exhibits superior robustness to variation in the amplifier gain (KA)compared to the PID controller as we can see the performance in Table 5.6.

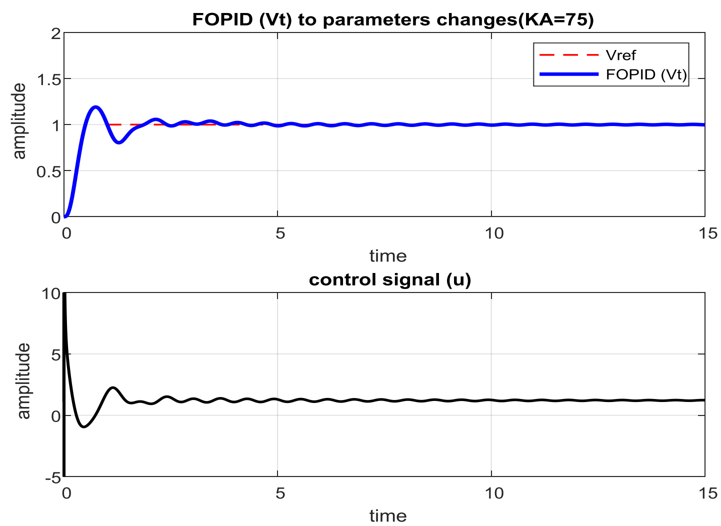

Figure 5. 8:Output Response of FOPID with Increased Amplifier gain

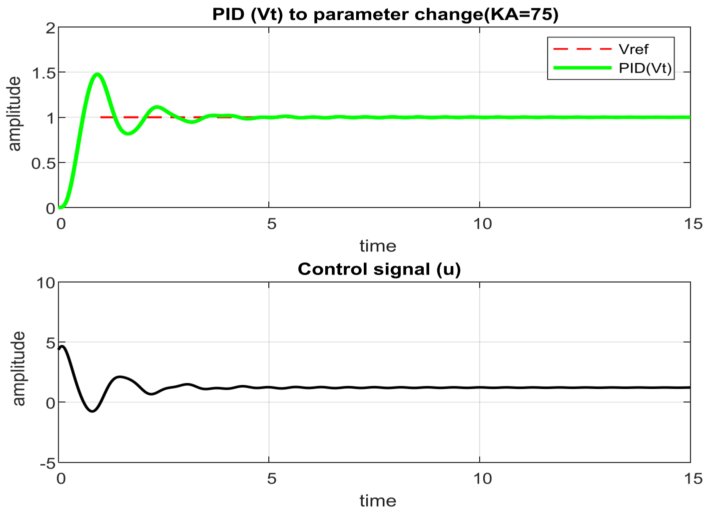

Figure 5. 9:Output Response of PID with Increased Amplifier gain

Table 5. 6:Performance Comparison Table for Increased Amplifier Gain

Controller	Performance Metrics				
	Settling time	Rise time	Maximum overshoot	Peak time	IAEU
FOPID	4.1213	**0.3099**	**19.0779**	**0.7440**	**2.4934**
PID	**3.3857**	0.3321	47.5761	0.9240	2.7126

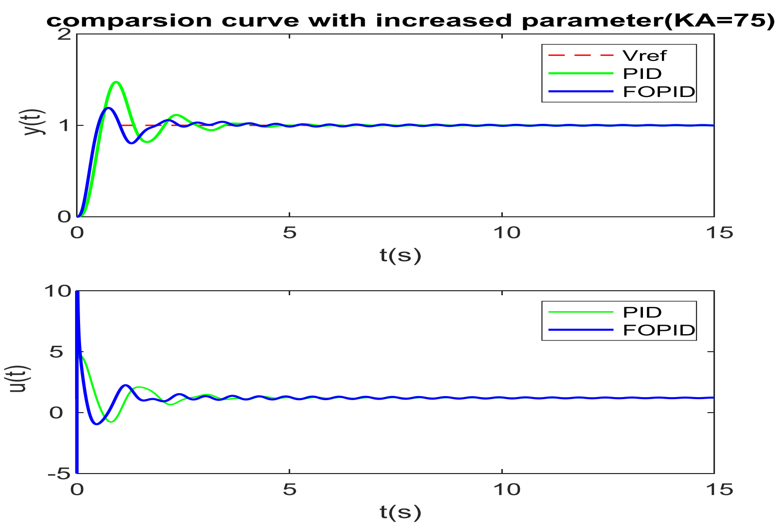

Figure 5. 10:Comparison plot of output response for increased amplifier gain

Case2: Decreased Amplifier Gain (-50%)

In this case the amplifier gain was reduced by 50% become 25pu value, both controllers experienced degraded performance compared to the nominal case. The FOPID controller showed a significant increase in settling time and peak time when compared to original value, indicating that it gives slower system response. In this case the proposed controller maintained better overshoot control (17.3753%) than that of PID controller (43.6178%). The PID controller also exhibited slower response with high overshoot and higher fitness cost, confirming its sensitivity to parameter variations. Overall, the FOPID controller remained more robust under this uncertainty, delivering comparatively smoother and more stable performance than the PID controller.

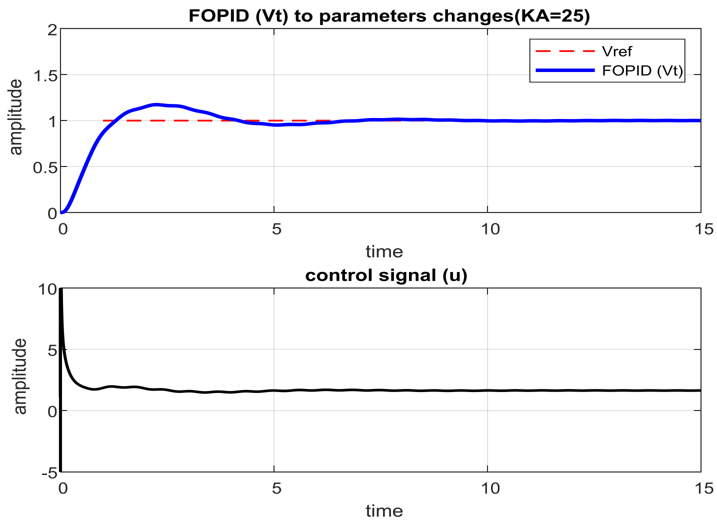

Figure 5. 11:Output Response of FOPID with Decreased Amplifier Gain

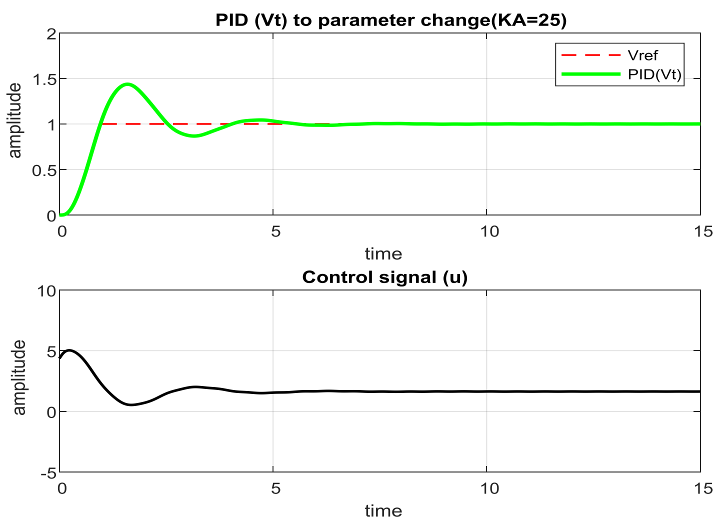

Figure 5. 12:Output Response of PID with Decreased Amplifier Gain

Table 5. 7:Performance Comparison Table for Decreased Amplifier Gain

Controller	Performance Metrics				
	Settling time	Rise time	Maximum overshoot	Peak time	IAEU
FOPID	6.3442	0.8354	**17.3753**	2.2520	**3.6788**
PID	**5.1877**	**0.5774**	43.6178	**1.5940**	3.8528

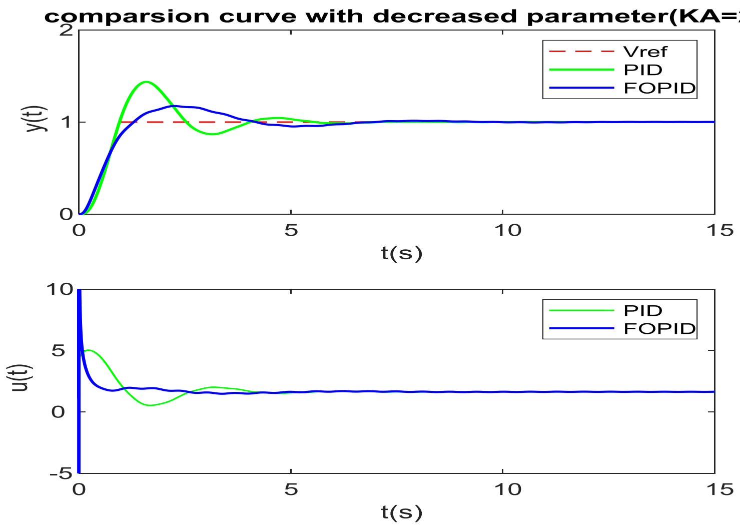

Figure 5. 13:Comparison plot of output response for decreased amplifier gain

5.4.2 Performance Tracking to Input Reference Change

The proposed GWO-optimized FOPID controller is tested against dynamic changes in the reference voltage. The input signal consisted of a positive step of 1 p.u start at t=0 to 2 seconds, decreased to 0.5 p.u. from 2 to 4 seconds, again increased to 1 p.u. for up to 6 seconds, declined to 0.5 p.u. up to 8 seconds, and finally remained constant at 1 p.u. thereafter. This dynamic reference scenario was used to check the performance of the controller to regulate frequent and sudden voltage changes. The tracking performance was tested for both the proposed FOPID controller and the PID controller as shown in Figure 5.14 and Figure 5.15. As we can see from Table 5.8 the FOPID controller demonstrates superior performance compared to the PID controller, exhibiting faster response, and having IAEU value 3.3676 lower than the PID 3.8005 indicating that gives a better tracking, especially in settling time and maximum overshoot.

Table 5. 8:Comparison Table of Performance Tracking to Change in Reference Input

Controller	Performance Metrics				
	Settling time	Rise time	Maximum overshoot	Peak time	IAEU
FOPID	**10.9705**	**0.4447**	**11.3970**	**0.9280**	**3.3676**
PID	11.0280	0.4056	46.6760	1.1000	3.8005

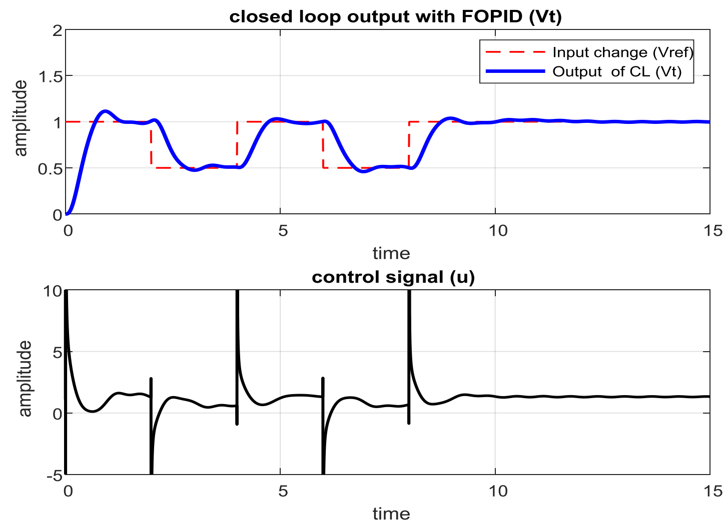

Figure 5. 14:Output response of GWO-FOPID to change in reference input

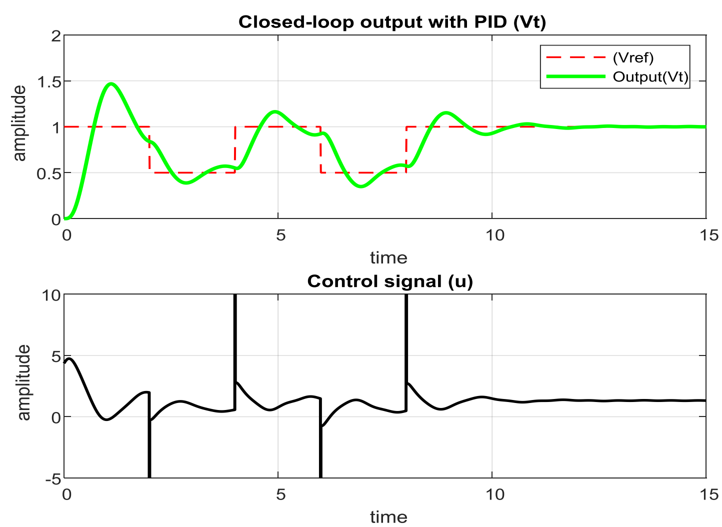

Figure 5. 15:Output response of Z-N tuned PID to change reference input

5.4.3 Performance Tracking to External Disturbance

The proposed GWO based FOPID controller was evaluated against the external disturbance, using change in delta Tm as step disturbance. This analysis is performed for two scenarios by introducing positive and negative step changes in delta Tm. Then the result is compared with the disturbance rejection capability of PID controller under identical disturbance condition.

Case1: Positive disturbance Tracking test

Figure 5.16 and 5.17 indicate the closed loop system's response to a positive disturbance scenario, where a positive step change of 3 p.u was introduced to the mechanical torque (delta Tm) at t=7 second. The plot shows how both controllers respond to this sudden increase in disturbance by showing the ability to maintain its terminal voltage regulation after in the phase of this external perturbation.

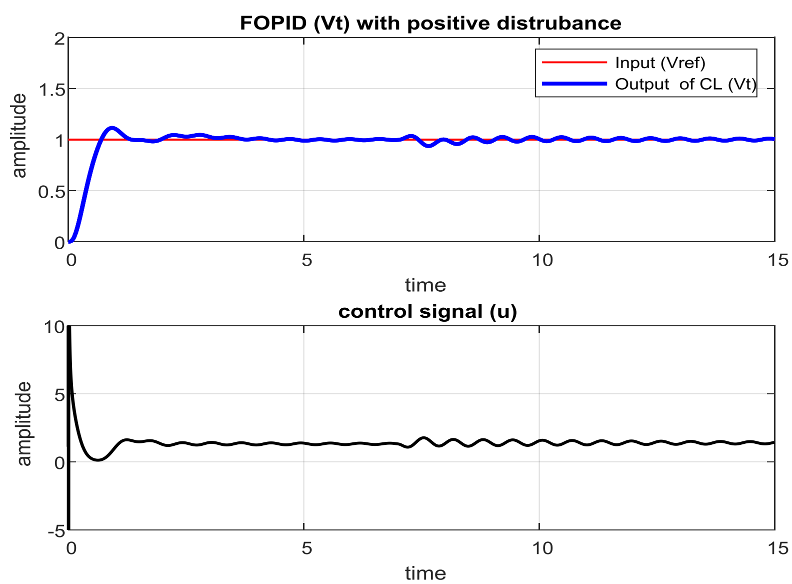

Figure 5. 16:Output response of GWO-FOPID under increased disturbance scenario

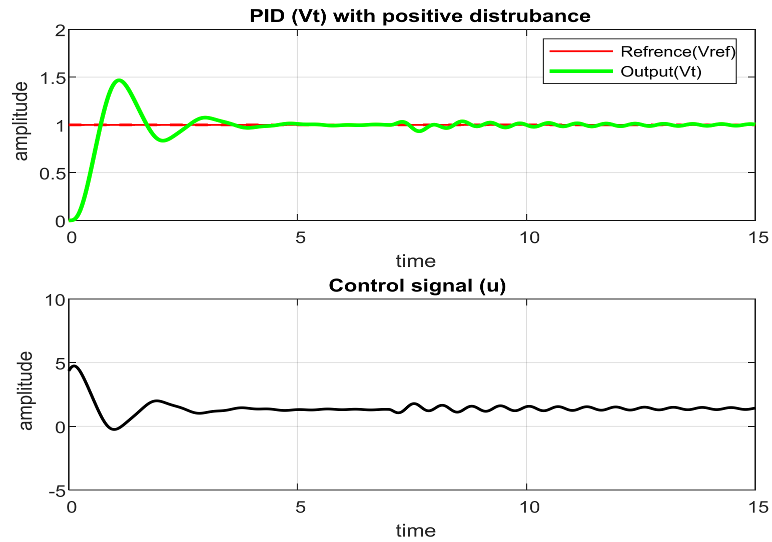

Figure 5. 17:Output response of PID under increased disturbance scenario

Under the positive disturbance scenario, both the proposed GWO-optimized FOPID controller and the PID controller shows a transient deviation in the terminal voltage following the introduction of the disturbance. However, the proposed FOPID controller demonstrates superior disturbance rejection with a smaller IAEU of 2.7495 and significantly reduced overshoot of 11.397% compared to the PID controller's that have 46.676% overshoot and higher IAEU of 3.1433. Figure 5.18 shows the comparison of the two controllers under positive disturbance case, by showing the performance metrics in the Table 5.9. Introducing the positive step disturbance to the closed loop system has led to increase the IAEU value for both controller and also the system takes longer to reach a stable steady-state after a disturbance.

Table 5. 9:Performance Tracking Comparison of Increased Disturbance Scenario

Controller	**Performance Metrics**				
	Peak time	Settling time	Maximum overshoot	Rise time	IAEU
FOPID	**0.9280**	10.5274	**11.397**	0.4470	**2.7495**
PID	1.1021	**10.5031**	46.676	**0.4056**	3.1433

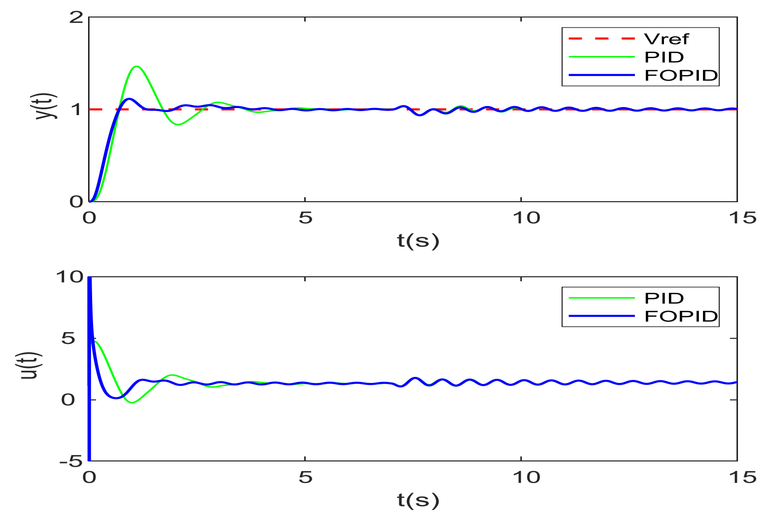

Figure 5. 18:Comparison plot of output response for increased disturbance scenario

Case2: Negative Disturbance Tracking test

Figure 5.19 and 5.20 indicate the closed loop system's response to a decreased disturbance scenario, where a negative step change of 3 p.u was introduced to the mechanical torque (delta Tm) at t=7 second. The plot shows how both controllers respond to this sudden decrease in disturbance by showing the ability to maintain its terminal voltage regulation after in the phase of this external perturbation.

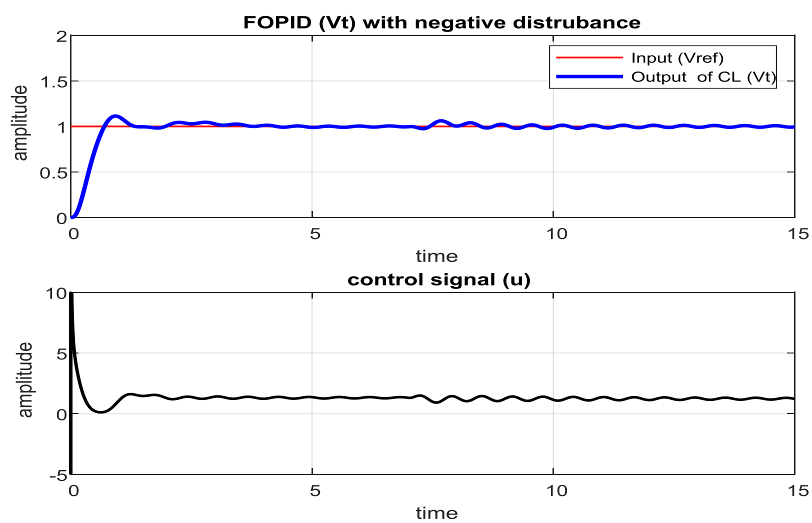

Figure 5. 19:Output response of GWO-FOPID for decreased disturbance scenario

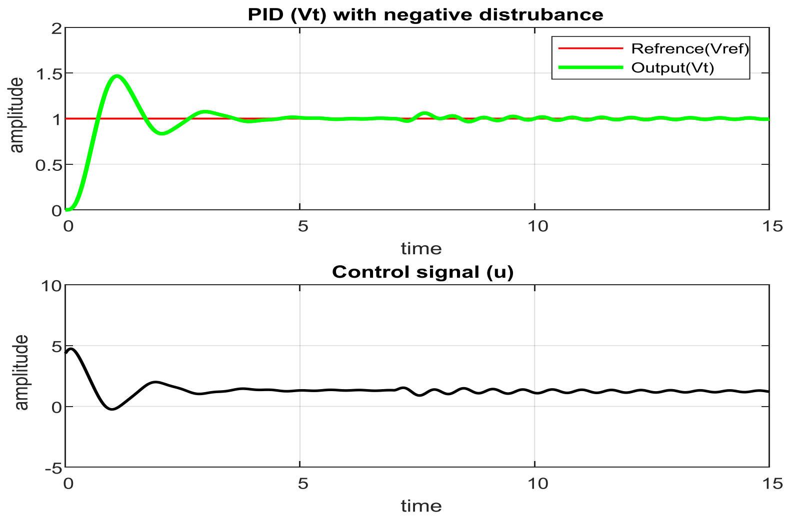

Figure 5. 20:Output response of PID for decreased disturbance scenario

Under the negative disturbance scenario, both the proposed GWO-optimized FOPID controller and the PID controller shows a transient deviation in the terminal voltage following the introduction of the disturbance but less when compared with that of positive disturbance scenario. However, the proposed GWO tuned FOPID controller demonstrates superior performance compared to the Z-N tuned PID controller in the negative disturbance scenario. Since it achieves a disturbance rejection with a smaller IAEU of 2.6157 and significantly reduced overshoot of 11.397% compared to the PID controller that have 46.670% overshoot. Despite the increased significant amount of rise time and settling time in the proposed system, a considerably shorter peak time of 0.928. Figure 5.21 can be depicted the comparison of the two controllers under negative disturbance case, by showing the performance metrics in Table 5.10. Introducing the negative step disturbance to the closed loop system has led to increase the IAEU value for both controllers and also the system takes longer to reach a stable steady-state after a disturbance. Generally, the negative disturbance scenario showed superior robustness compared to the positive disturbance scenario, even exhibiting smaller values across all performance metrics.

Table 5. 10:Performance Tracking Comparison of Decreased Disturbance Scenario

Controller	Performance Metrics				
	Rise time	Settling time	Maximum overshoot	Peak time	IAEU
FOPID	0.4447	10.5036	**11.3970**	**0.9280**	**2.6157**
PID	**0.4056**	**9.6066**	46.670	1.1000	3.0088

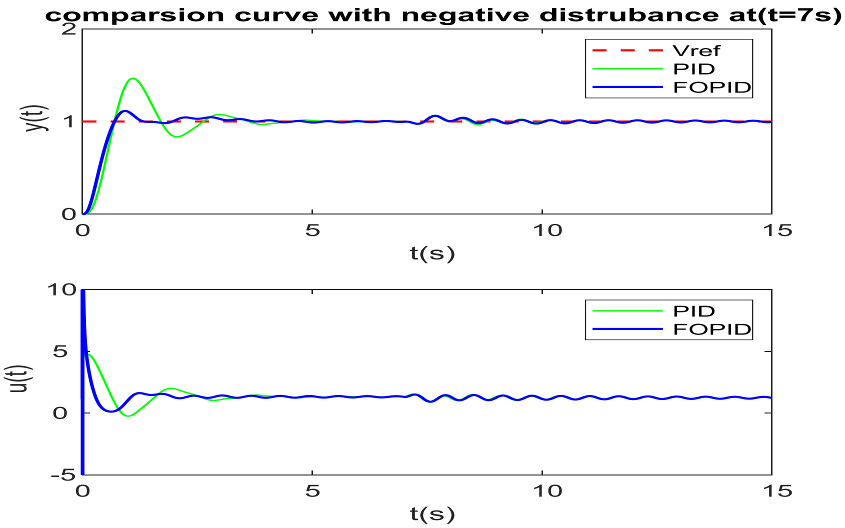

Figure 5. 21:Comparison plot of closed-loop response for decreased disturbance scenario

CHAPTER SIX

6.CONCLUSION AND RECOMMENDATION

6.1 Conclusion

This research investigates the application of grey wolf optimization based fractional order PID controller for voltage regulation of synchronous generator. The linearized dynamic model of the synchronous generator is developed. Following the formulation of the system, to achieve improved control accuracy and dynamic performance, a FOPID controller was employed, and further flexibility was obtained by introducing fractional orders in the integral and derivative terms. Grey Wolf Optimization was employed to tune the parameters of FOPID in a systematic manner, attempting to minimize integral performance indices and enhance voltage regulation accuracy.

The efficiency and performance of the designed controller is tested for voltage regulation of synchronous generator using MATLAB/Simulink software environment by introducing external disturbance at t=7second (i.e., use mechanical toque as disturbance) and parameter uncertainty (change in amplifier gain, KA).The proposed system exhibits significant performance improvement over a Z-N tuned PID controller, achieving faster settling time of 3.541 second, reduced overshoot of 11.397%, and a lower IAEU tracking error of 2.5963.

In general, these findings confirm that the superiority of the GWO-optimized FOPID controller in enhancing synchronous generator voltage regulation. In addition, due to its great accuracy, flexibility, and high robustness potential, the proposed method has extremely good prospects for practical implementation in modern power systems.

6.2 Recommendation

This study suggests the following points for future researcher:

- To include the adaptive or self-tuning concept for enhance performance under varying load and nonlinear operating conditions.

- To evaluate the effectiveness of the FOPID controller by simulating the synchronous generator model on a grid-connected system and add hardware implementation.

RESEARCH FUND ACKNOWLEDGMENT

This thesis work is funded by ASTU under grant number ASTU/SM-R/1107/25.

REFERENCES

Abbas, F., Saleem, O., Wang, L., & Yan, Y. (2024). A self-adaptive fractional-order PID controller for the particle velocity regulation in a pneumatic conveying system. *Transactions of the Institute of Measurement and Control*. https://doi.org/10.1177/01423312241277592

Anwar, N., Hanif, A., Ali, M. U., & Zafar, A. (2021). Chaotic-based particle swarm optimization algorithm for optimal PID tuning in automatic voltage regulator systems. *Electrical Engineering & Electromechanics*, *1*, 50–59. https://doi.org/10.20998/2074-272X.2021.1.08

babu, F. A. G. S., & Chiranjeevi, S. B. T. (2016). Implementation of Fractional Order PID Controller for an AVR System Using GA and ACO Optimization Techniques. *IFAC-PapersOnLine*, *49*(1), 456–461. https://doi.org/10.1016/j.ifacol.2016.03.096

Bhullar, A. K., Kaur, R., & Sondhi, S. (2020). Design of FOPID Controller for Optimizing AVR System using Neural Network Algorithm. *2020 IEEE 17th India Council International Conference (INDICON)*, 1–7. https://doi.org/10.1109/INDICON49873.2020.9342274

Brezovec, M., Kuzle, I., & Krpan, M. (2022). Detailed mathematical and simulation model of a synchronous generator. *Journal of Energy - Energija*, *64*(1–4), 102–129. https://doi.org/10.37798/2015641-4147

Ellis, G. (2012). Four Types of Controllers. In *Control System Design Guide* (pp. 97–119). Elsevier. https://doi.org/10.1016/B978-0-12-385920-4.00006-0

Ezenugu, I. A., & Nwokonko, C. S. (2024). Automatic Voltage Regulator Control System for Synchronous Generator. *Saudi Journal of Engineering and Technology*, *9*(06), 265–273. https://doi.org/10.36348/sjet.2024.v09i06.004

Hadi Saadat. (1999). *Power System Analysis* (J. Betsy & C. Lynn, Eds.). Kevin Kane.

Hang, C. C., Astrom, K. J., & Wang, Q. G. (2002). Relay feedback auto-tuning of process controllers — a tutorial review. *Journal of Process Control*, *12*(1), 143–162. https://doi.org/10.1016/S0959-1524(01)00025-7

Hekimoğlu, B. (2019). Sine-cosine algorithm-based optimization for automatic voltage regulator system. *Transactions of the Institute of Measurement and Control*, *41*(6), 1761–1771. https://doi.org/10.1177/0142331218811453

Ibraheem Kasim Ibraheem. (2011). A Digital-Based Optimal AVR Design of Synchronous Generator Exciter Using LQR Technique. *Al-Khwarizmi Engineering Journal*, *7*(1), 82–94.

Ibrahim, M. M., Jiya, J. D., & Harrison, I. O. (2017). Modelling and Simulation of Automatic Voltage Regulator System General Terms. In *International Journal of Computer Applications* (Vol. 178, Issue 1).

Khan, I. A., Alghamdi, A. S., Jumani, T. A., Alamgir, A., Awan, A. B., & Khidrani, A. (2019). Salp Swarm Optimization Algorithm-Based Fractional Order PID Controller for Dynamic Response and Stability Enhancement of an Automatic Voltage Regulator System. *Electronics*, *8*(12), 1472. https://doi.org/10.3390/electronics8121472

KUNDUR, P. (1994). *Power System Stability and Control* (Neal J.Balu & Mark G.Lauby, Eds.; Vol. 1). McGraw-Hill,Inc.

Li, X., Wang, Y., Li, N., Han, M., Tang, Y., & Liu, F. (2017). Optimal fractional order PID controller design for automatic voltage regulator system based on reference model using particle swarm optimization. *International Journal of Machine Learning and Cybernetics*, *8*(5), 1595–1605. https://doi.org/10.1007/s13042-016-0530-2

Micev, M., Ćalasan, M., & Oliva, D. (2020). Fractional Order PID Controller Design for an AVR System Using Chaotic Yellow Saddle Goatfish Algorithm. *Mathematics*, *8*(7), 1182. https://doi.org/10.3390/math8071182

Mirjalili, S., Mirjalili, S. M., & Lewis, A. (2014). Grey Wolf Optimizer. *Advances in Engineering Software*, *69*, 46–61. https://doi.org/10.1016/j.advengsoft.2013.12.007

Mohammad Ali Daftari, & Mohammad Ali Nekoui. (2018). Analysing Stability of Time Delayed Synchronous Generator and Designing Optimal Stabilizer Fractional Order PID Controller using Partical Swarm Optimization Technique. *2nd IEEE International Conference on Power Electronics, Intelligent Control and Energy Systems (ICPEICES-2018).*

Mohd Tumari, M. Z., Ahmad, M. A., Suid, M. H., & Hao, M. R. (2023). An Improved Marine Predators Algorithm-Tuned Fractional-Order PID Controller for Automatic Voltage Regulator System. *Fractal and Fractional*, *7*(7), 561. https://doi.org/10.3390/fractalfract7070561

Mosaad, A. M., Attia, M. A., & Abdelaziz, A. Y. (2019). Whale optimization algorithm to tune PID and PIDA controllers on AVR system. *Ain Shams Engineering Journal*, *10*(4), 755–767. https://doi.org/10.1016/j.asej.2019.07.004

Nataraj, D., & Subramanian, M. (2025). Design and optimal tuning of fractional order PID controller for paper machine headbox using jellyfish search optimizer algorithm. *Scientific Reports*, *15*(1), 1631. https://doi.org/10.1038/s41598-025-85810-9

Oladipo, S., Sun, Y., & Wang, Z. (2020). 2 th International Conference on Computational Intelligence and Communication Networks Optimization of PID and FOPID controllers with new generation metaheuristic algorithms for controlling AVR system: Concise Survey. *2020 12th International Conference on Computational Intelligence and Communication Networks (CICN)*. https://doi.org/10.1109/CICN.2020.52

Özdemir, M., & ÇELİK, V. (2017). Stability analysis of the automatic voltage regulation system with PI controller. *SAÜ Fen Bilimleri Enstitüsü Dergisi*, 1–1. https://doi.org/10.16984/saufenbilder.270251

Podlubny, I. (1999). Fractional-order systems and PI/sup /spl lambda//D/sup /spl mu//-controllers. *IEEE Transactions on Automatic Control*, *44*(1), 208–214. https://doi.org/10.1109/9.739144

Ramezanian, H., Balochian, S., & Zare, A. (2013). Design of Optimal Fractional-Order PID Controllers Using Particle Swarm Optimization Algorithm for Automatic Voltage Regulator

(AVR) System. *Journal of Control, Automation and Electrical Systems*, *24*(5), 601–611. https://doi.org/10.1007/s40313-013-0057-7

Ribeiro, R. L. A., Neto, C. M. S., Costa, F. B., Rocha, T. O. A., & Barreto, R. L. (2015). A sliding-mode voltage regulator for salient pole synchronous generator. *Electric Power Systems Research*, *129*, 178–184. https://doi.org/10.1016/j.epsr.2015.07.016

Salih, A. M., Humod, A. Th., & Hasan, F. A. (2019). Optimum Design for PID-ANN Controller for Automatic Voltage Regulator of Synchronous Generator. *2019 4th Scientific International Conference Najaf (SICN)*, 74–79. https://doi.org/10.1109/SICN47020.2019.9019367

Stephen J.Chapman. (2005). *Electric Machiner Fundamentals* (P. Carlise, Ed.; 4th ed., Vol. 4). Elizabeth A. Jones.

Tepljakov, A., Petlenkov, E., & Belikov, J. (2019). FOMCON toolbox for modeling, design and implementation of fractional-order control systems. In *Applications in Control* (pp. 211–236). De Gruyter. https://doi.org/10.1515/9783110571745-010

Türksoy, Ö., & Türksoy, A. (2024). A fast and robust sliding mode controller for automatic voltage regulators in electrical power systems. *Engineering Science and Technology, an International Journal*, *53*, 101697. https://doi.org/10.1016/j.jestch.2024.101697

Vanço, W. E., Silva, F. B., Oliveira, J. M. M., & Almeida Monteiro, J. R. B. (2020). Effects of harmonic pollution on salient pole synchronous generators and on induction generators operating in parallel in isolated systems. *International Transactions on Electrical Energy Systems*, *30*(6). https://doi.org/10.1002/2050-7038.12359

Verma, S. K., Yadav, S., & Nagar, S. K. (2017). Optimization of Fractional Order PID Controller Using Grey Wolf Optimizer. *Journal of Control, Automation and Electrical Systems*, *28*(3), 314–322. https://doi.org/10.1007/s40313-017-0305-3

APPENDIXES

Appendix A1: Simulink model of feedback relay tuned PID controller

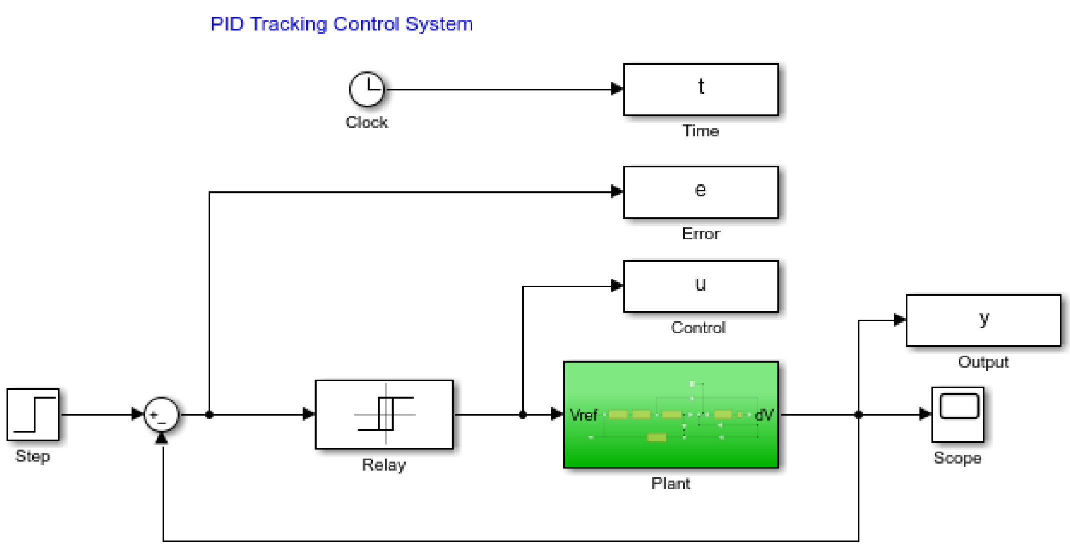

Appendix A2: Simulink model of AVR of the synchronous generator

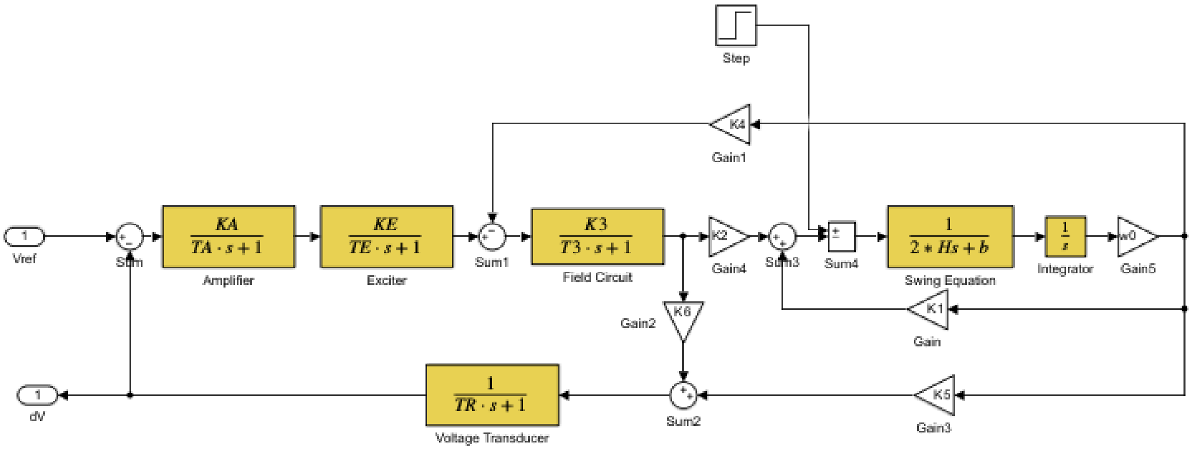

Appendix B1

```
%%MATLAB CODE FOR GWO
clc;
clear all;
rng(1234) % Initialize the random number generator
%% Step 2: GWO Parameters

SearchAgents_no = 20;
Max_iter = 10;
% Lower and upper bounds [Kp Ki Kd lambda mu]
lb = [0 0 0 0 0];
ub = [5 5 5 2 2];
% Run GWO
[Best_pos, Best_score, Convergence_curve] = GWO(SearchAgents_no, Max_iter, lb, ub, fobj);
% Display best FOPID params
disp('Best FOPID Parameters from GWO:');
```

```
Kp = Best_pos(1); Ki = Best_pos(2); Kd = Best_pos(3); lambda = Best_pos(4); mu =
Best_pos(5);
disp(["Kp", Kp; "Ki", Ki; "Kd", Kd; "lambda", lambda; "mu", mu]);
%% --- Function: Grey Wolf Optimizer ---
function [Alpha_pos, Alpha_score, Convergence_curve] = GWO(SearchAgents_no, Max_iter,
lb, ub, fobj)
  dim = length(lb);
  Alpha_pos = zeros(1, dim); Alpha_score = inf;
  Beta_pos = zeros(1, dim); Beta_score = inf;
  Delta_pos = zeros(1, dim); Delta_score = inf;
  Positions = rand(SearchAgents_no, dim) .* (ub - lb) + lb;
  Convergence_curve = zeros(1, Max_iter);
for l = 1:Max_iter
for i = 1:SearchAgents_no
      Positions(i,:) = max(min(Positions(i,:), ub), lb);
      fitness = fobj(Positions(i,:));
if fitness < Alpha_score
        Alpha_score = fitness; Alpha_pos = Positions(i,:);
elseif fitness < Beta_score
        Beta_score = fitness; Beta_pos = Positions(i,:);
elseif fitness < Delta_score
        Delta_score = fitness; Delta_pos = Positions(i,:);
end
end
    a = 2 - l * (2 / Max_iter);
for i = 1:SearchAgents_no
for j = 1:dim
        r1 = rand(); r2 = rand();
        A1 = 2 * a * r1 - a; C1 = 2 * r2;
        D_alpha = abs(C1 * Alpha_pos(j) - Positions(i,j));
        X1 = Alpha_pos(j) - A1 * D_alpha;
```

```
            r1 = rand(); r2 = rand();
            A2 = 2 * a * r1 - a; C2 = 2 * r2;
            D_beta = abs(C2 * Beta_pos(j) - Positions(i,j));
            X2 = Beta_pos(j) - A2 * D_beta;
            r1 = rand(); r2 = rand();
            A3 = 2 * a * r1 - a; C3 = 2 * r2;
            D_delta = abs(C3 * Delta_pos(j) - Positions(i,j));
            X3 = Delta_pos(j) - A3 * D_delta;
            Positions(i,j) = (X1 + X2 + X3) / 3;
end
end
    Convergence_curve(l) = Alpha_score;
    disp(["Iteration", l, "Best Fitness", Alpha_score]);
end
end
```